EVALUATION OF FUEL SAVINGS DUE TO POWERTRAIN ELECTRIFICATION OF CLASS 8 TRUCKS

A Thesis

Submitted to the Faculty

of

Purdue University

by

Sree Harsha Rayasam

In Partial Fulfillment of the

Requirements for the Degree

of

Master of Science in Mechanical Engineering

December 2018

Purdue University

West Lafayette, Indiana

THE PURDUE UNIVERSITY GRADUATE SCHOOL
STATEMENT OF THESIS APPROVAL

Dr. Gregory M. Shaver, Chair

School of Mechanical Engineering

Dr. Peter H. Meckl

School of Mechanical Engineering

Dr. Neera Jain

School of Mechanical Engineering

Approved by:

Dr. Jay P. Gore

Head of the Departmental Graduate Program

To my parents and my brother

ACKNOWLEDGMENTS

I would like to very sincerely thank my advisor, Dr. Greg Shaver for his invaluable guidance and support throughout my research and coursework. I would like to thank Dr. Peter Meckl and Dr. Neera Jain for serving on my committee and providing helpful feedback on my thesis. I am thankful to Dr. Galen King and Dr. George Chiu for their advice that helped me become a better TA. I would also like to thank the School of Mechanical Engineering for providing financial aid in the form of teaching assistantships during the course of this work. I am thankful to Vaidehi and Sharon for their contributions without which this thesis would be incomplete.

Most importantly, I am extremely thankful to my parents and my brother for their encouragement, support and belief in me that has brought me this far.

TABLE OF CONTENTS

LIST OF TABLES

LIST OF FIGURES

ABBREVIATIONS

CI	Compression Ignition
ECM	Engine Control Module
ESS	Energy Storage System
GHG	Greenhouse gas
GVW	Gross Vehicle Weight
HEV	Hybrid Electric Vehicle
ICE	Internal Combustion Engine
IFTA	International Fuel Tax Agreement
LHV	Lower Heating Value
PHEV	Plug0in Hybrid Electric vehicle
SOC	State of Charge
US EPA	United States Environmental Protection Agency
VPA	Vehicle Powertrain Architecture
VPC	Vehicle Powertrain Controller

ABSTRACT

Rayasam, Sree Harsha M.S.M.E, Purdue University, December 2018. Evaluation of Fuel Savings due to Powertrain Electrification of Class 8 Trucks. Major Professor: Gregory M. Shaver, School of Mechanical Engineering.

Ever-increasing need for freight transportation and mounting environmental concerns call for a cleaner and more efficient energy source. Hybrid electric vehicles have shown potential to reduce both petroleum usage as well as harmful emissions. In this thesis, a newly developed series hybrid electric powertrain by a small start-up company is studied on a route between Florence, Kentucky and Cambridge, Ohio hubs to evaluate potential fuel savings due to hybridization.

An experimental testing protocol to calculate fuel economy has been developed and the real-world fuel economy of this hybrid electric powertrain is calculated. A vehicle simulation model representing the experimental powertrain is created in Autonomie and this vehicle model is simulated on three distinct drive cycles obtained from experimental testing phase. These results are compared with a conventional class 8 truck to evaluate fuel savings. The simulation analysis indicates that fuel economy of hybrid is better on only one of the three drive cycles under consideration. Further, it is determined that the existing powertrain does not meet the gradeability criterion. To remedy this, a series electric hybrid powertrain with different component sizes is then modeled and simulated on the same drive cycles. The modified powertrain is found to result in fuel economy improvement on all three drive cycles considered while also meeting the gradeability requirement. The effect of drive cycle on fuel economy of a hybrid powertrain is also studied in this thesis.

1. INTRODUCTION

1.1 Motivation

Climate change poses a serious threat to the world as we know it. The alarming rate of the rise in Earth's surface temperature is evident from Figure 1.1 ([1]). According to [2], 17 of the 18 warmest years in 136 year record have occurred since 2001. Rising sea levels and unstable ecosystems are a few of the potential long term repercussions. A major contributor to this severe climate change is an increase in greenhouse gas (GHG) emissions into the Earth's atmosphere.

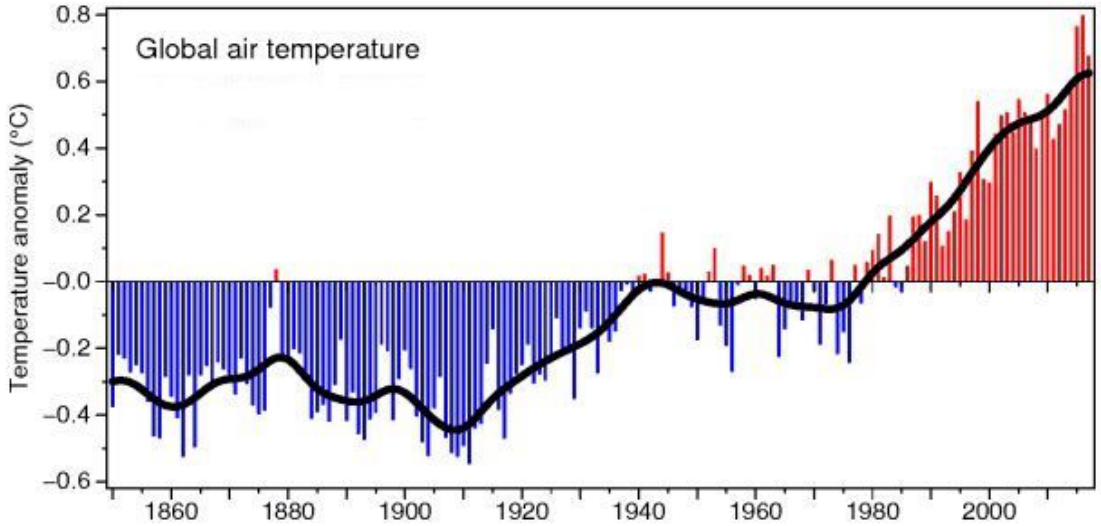

Figure 1.1. Global air temperature at surface.

The transportation sector is one of the chief economic sectors that has a direct causal link to the increase in GHG emissions. This issue is shown in Figure 1.2. Within the transportation sector, which is composed of different classes of vehicles, the energy consumption by medium-duty and heavy-duty vehicles are projected to steadily increase over time [3] (shown in Figure 1.3). In an effort to reduce GHG

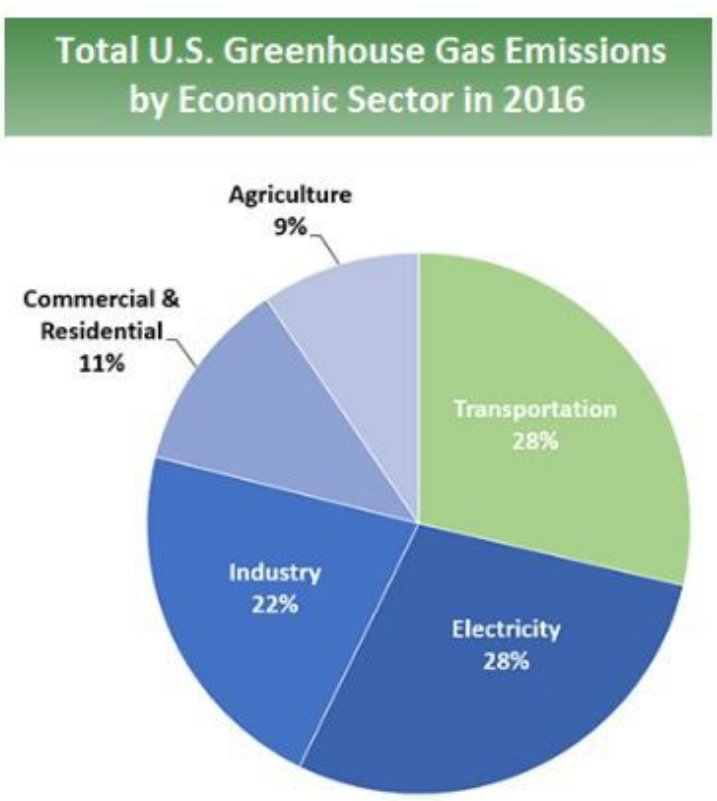

Figure 1.2. Greenhouse gas emissions by various economic sectors.

emissions from automobiles, the United States Environmental Protection Agency (US EPA) has set new standards (Phase 2) that are expected to increase fuel economy of automobiles and hence reduce emissions. A graph that shows these new standards for fuel economy is depicted in Figure 1.4.

Powertrain electrification is a promising technology that would enable better fuel economy while reducing GHG emissions. This technology fundamentally aims to reduce fuel consumption by operating the conventional internal combustion engine (ICE) as efficiently as possible while consuming energy from the battery, when needed.

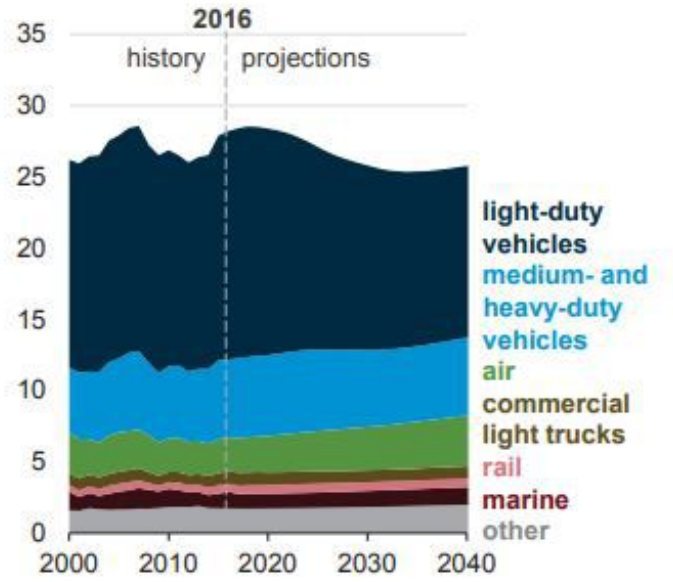

Figure 1.3. Energy consumption by different classes of vehicles.

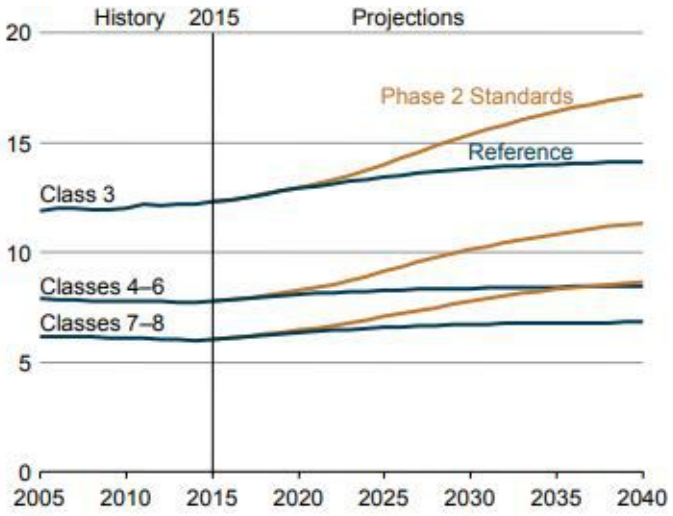

Figure 1.4. Fuel economy standards by US EPA.

1.2 Hybrid Powertrain Architectures

Hybrid electric vehicles (HEV) use a combination of conventional ICE and battery pack for propulsion. Due to this, a HEV can be operated in various ways, namely

battery only, engine only, or combined mode based on the power demand. Different powertrain architectures of HEVs are possible based on the manner in which the components in the powertrain are connected together. A few primary architectures are discussed briefly below [4]:

1.2.1 Series Hybrid Architecture

Figure 1.5 shows a series hybrid electric architecture. In a series HEV, the ICE is the main energy converter that converts fuel energy into mechanical power that can used be used for propulsion. The electric motor then propels the vehicle using this energy from the generator and/or the battery. Since the engine is decoupled from the wheels, it can be operated at its optimum speed as long as the required power is being supplied to meet the vehicle power demand. This feature also simplifies the control of the engine in a series HEV. Since all of the power is finally delivered through the motor, that motor peak power has to be high enough so that it can actually deliver all the required power.

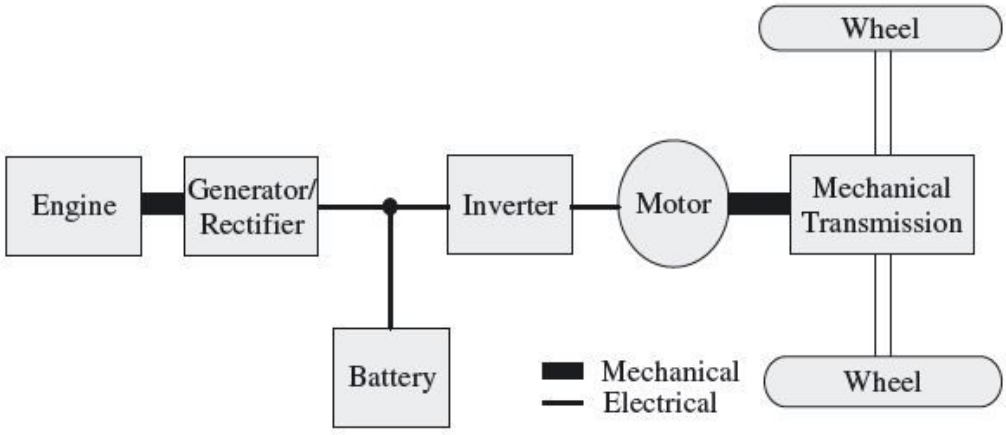

Figure 1.5. Series hybrid architecture.

1.2.2 Parallel Hybrid Architecture

A parallel hybrid architecture is depicted in Figure 1.6. In this architecture, the motor and ICE are coupled with a mechanical coupling (clutch, gear, belt, pulley etc.). Within a parallel architecture, different architectures such as pre-transmission parallel hybrid or a post-transmission parallel hybrid architectures are possible depending on where the transmission is placed with respect to the coupling between motor and engine. Since the motor is no longer the bottleneck in terms of power, a smaller engine and motor can be selected when using this architecture. However, this needs a more complex control system as compared to a series HEV architecture.

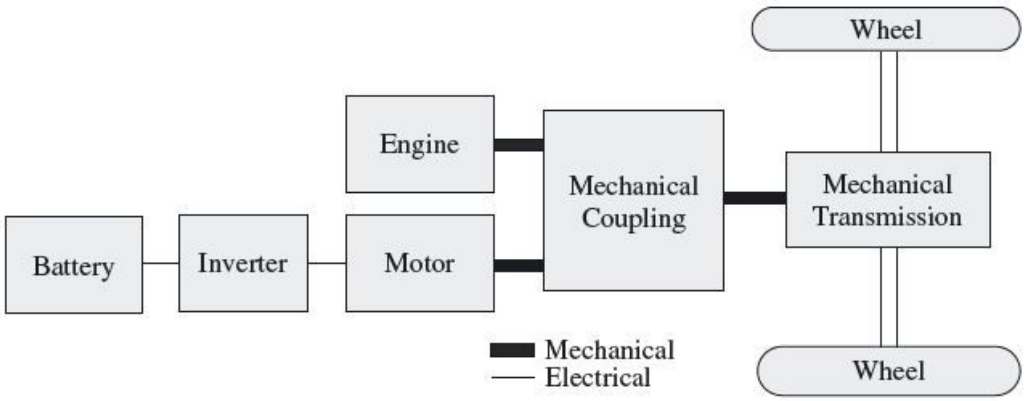

Figure 1.6. Parallel hybrid architecture.

1.2.3 Other Methods of Hybridization

Other architectures, like a series-parallel architecture and complex architectures involving the use of planetary gear systems or multiple electric motors are also possible. In a series-parallel architecture, the vehicle can be operated in either series or parallel mode. Because of this, the fuel efficiency and drivability can be optimized based on vehicle's operating condition. Nevertheless, due to greater complexity, this architecture is generally more expensive compared to a series or a parallel archi-

tecture. Plug-in HEVs (PHEVs) can be recharged using the electric grid whenever needed. This further reduces the fuel consumption as the battery can be used without maintaining its state of charge (SOC). This is not the case in a HEV as there is no option to recharge the battery after usage and therefore the SOC in a HEV has to be maintained during operation.

In all of these HEV architectures mentioned before, a feature that plays a vital role in potentially obtaining a better fuel economy is regenerative braking [5]. This is principally being able to capture some of the kinetic energy that is available during braking, which otherwise would have been wasted in a conventional powertrain. In order to capture a part of the braking energy available, the electric motor operates as a generator and converts the kinetic energy of the vehicle into electrical energy that can be stored in the battery for future usage. The benefit of regenerative braking is most evident in stop-and-go traffic since there are more opportunities for braking and capturing some of that braking energy. Although regenerative braking is possible in highway driving conditions as well, the number of braking opportunities in such conditions are significantly lower than in city driving conditions. This, along with an ability to switch off the engine at low loads are the primary reasons why higher fuel savings can be realized in drive cycles with stops as compared to highway style drive cycles [6].

Since there are two power sources in a HEV, a great amount of research has been conducted on developing an optimal power management control strategy for the powertrain. In [7], an Equivalent Consumption Minimization Strategy (ECMS) has been used to compute the optimum power split between engine and battery. Some control strategies are designed in order to minimize an objective function (for example, fuel consumption) and these strategies make use of dynamic programming (DP) and Pontryagin's minimum principle (PMP) [8]. However, these control strategies require the knowledge of the entire drive cycle in advance and hence cannot be implemented in real time. [9] proposes a stochastic model predictive method with on-board learning to optimize fuel economy by modeling the driver power demand as a Markov chain.

1.3 Objective of the Work and Thesis Distribution

The work compiled to form this thesis is divided into two phases:

Phase 1: The objective of the work done in this phase is to determine the fuel consumption impact of a class 8 prototype truck with a series electric hybrid powertrain developed by a small start-up company. The fuel consumption data collected, along with the testing procedures, have been documented into a report in detail.

Phase 2: The second phase of the work consisted of developing a vehicle simulation model to provide further insight into the operation of the powertrain and aid in determining any shortcomings and also potential scope for improvement.

Chapter 2 details the work done during phase 1. It is followed by chapter 3, which details the vehicle simulation model along with the simulation results. Chapter 4 marks the conclusion of the thesis along with a brief discussion of the scope for future work.

2. EXPERIMENTAL TESTING OF THE PROTOTYPE TRUCK

In order to determine the fuel consumption of the prototype truck, several real world tests were performed between June 2017 and November 2017 on the route from Florence, Kentucky to Cambridge, Ohio. The fuel economy of the truck for all of the tests performed is reported in miles/kg instead of miles/gallon in order to eliminate the effect of variation of density of diesel. The difference in odometer reading before and after the test gives the number of miles/kilometers and the difference in the weight of the fuel tank before and after the test gives the number of pounds/kilograms of diesel used during the test.

The powertrain in the prototype truck is a series electric hybrid and the table below (Table 2.1) lists the individual component details.

Table 2.1. Powertrain - Prototype truck.

Powertrain Component	**Model**
Engine	Cummins ISB 6.7L Compression Ignition (CI) Engine
Electric Motor	Marathon Mariner Electric Motor
Battery	46 NiMH cells in series
Transmission	Eaton Ultra Shift 10 Speed RTO-16910

2.1 Real World Fuel Economy Testing of The Truck

The fuel economy testing process broadly consists of two parts:

(i) Calibration of the weight of the fuel tank, performed one day prior to the actual testing of the truck.

(ii) On-road testing of the truck

Even though numerous tests were performed on the same route, the test that was performed on 27 June, 2017 is described in detail in this section to avoid repetition. The To and Return routes for this test, as plotted by Google maps are shown in Figures 2.1 and 2.2, respectively.

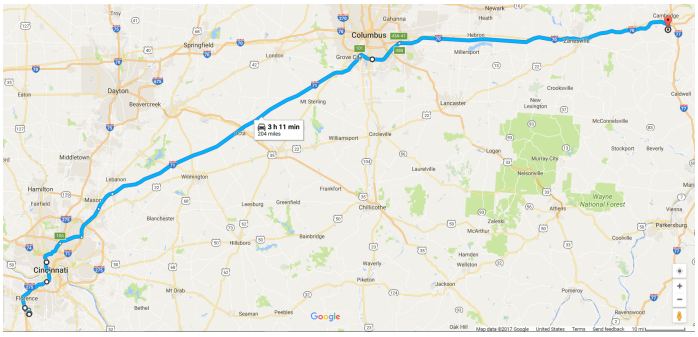

Figure 2.1. To route.

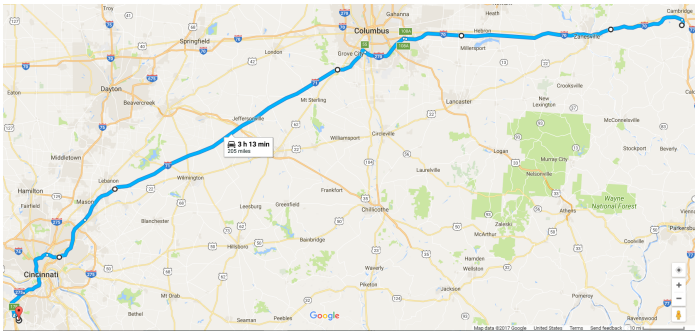

Figure 2.2. Return route.

2.1.1 Calibration and Installation of the Fuel Tank

The first step in the calibration of the weight of the fuel tank is to measure the weight of the empty test fuel tank. This step was completed on 26 June, 2017, the

day before the actual on-road testing of the truck. Figure 2.3 shows the weighing scale with a reading of zero without any load. The fuel tank is disassembled from the tractor and is placed on the weighing scale using a wooden platform as shown in Figure 2.4. The weight of the empty fuel tank + wooden platform, shown in Figure 2.5 is noted.

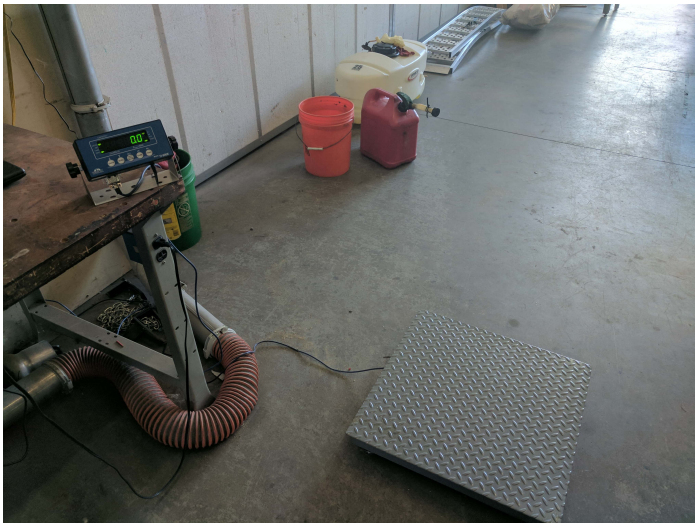

Figure 2.3. Weighing scale used to calibrate the weight of the fuel tank.

Figure 2.4. Empty fuel tank, wooden pallet on weighing scale.

Figure 2.5. Weight of the empty fuel tank + wooden pallet.

Since all the diesel cannot be pumped out of the fuel tank while emptying it, some of it would always be left over in the tank when it is being weighed. This small amount of diesel that is left over in the fuel tank (see Figure 2.6) is already accounted for while measuring the weight of the "empty" fuel tank and therefore, this left over diesel does not affect the calculation of the amount of fuel that would be used during the testing of the truck.

The prototype hybrid tractor has two fuel tanks, a 70-gallon capacity tank which is the test fuel tank and 40-gallon capacity tank which is installed so that it could be used in emergency situations (for example, an empty test fuel tank due to unforeseen circumstances). A photo of emergency fuel tank is shown in Figure 2.7 and the slot for test tank is shown in Figure 2.8.

By using two three-way ball valves which are manually operated, one for suction to the engine and one for return from the engine (shown in Figure 2.9), the plumbing connection of engine can be shifted from one tank to the other by altering the position of the handle of three-way valve. A picture of one of the three-way valves is shown in Figure 2.10. In order to be certain that fuel is being used from the test fuel tank

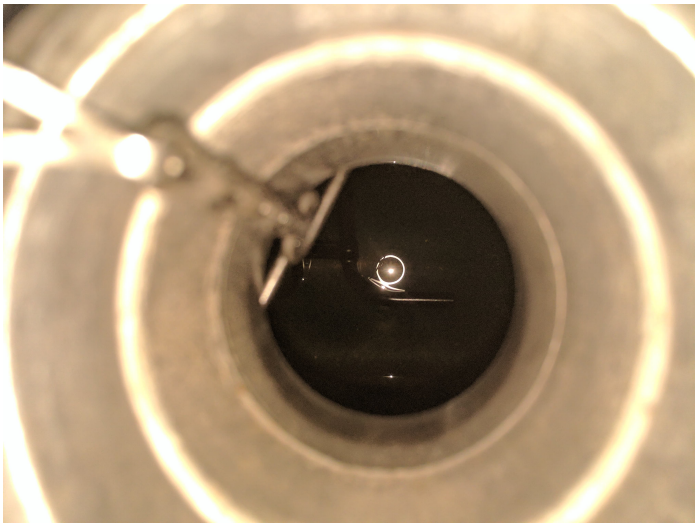

Figure 2.6. Residual in-tank fuel.

Figure 2.7. Emergency fuel tank.

and not the emergency fuel tank during the actual testing, the plumbing connections to the engine are checked before testing the truck on road.

Even though the handles of both three-way valves are positioned in such a way that the fuel can be used only from the test fuel tank, completely disconnecting the emergency fuel tank from the engine by removing the plumbing connections would be

Figure 2.8. Slot for test fuel tank.

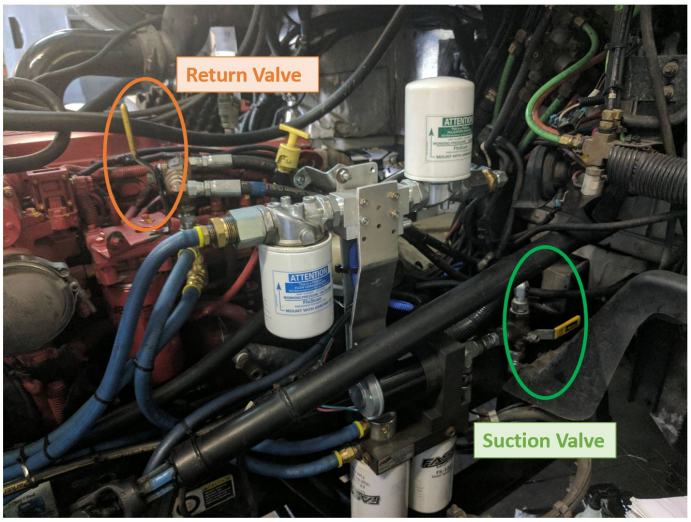

Figure 2.9. Suction valve and return valve.

better because there would be no way for the engine to use fuel from the emergency fuel tank even if there is any minor leakage within the three-way valves. The suction and return valves after disconnecting the engine from the emergency fuel tank are shown in Figures 2.11 and 2.12 respectively. In Figure 2.11, it can be noticed that there is only one fuel pipe (one which is connected to the test tank) that is actually

Figure 2.10. Three-way valve used to shift plumbing connection to the engine.

connected to the suction valve. Similarly, in Figure 2.12, it can be noticed that there is only one fuel pipe (one which is connected to the test tank) that is actually connected to the return valve. Therefore, this ensures that all fuel that would be used during the test could only be from the test tank and not the emergency tank.

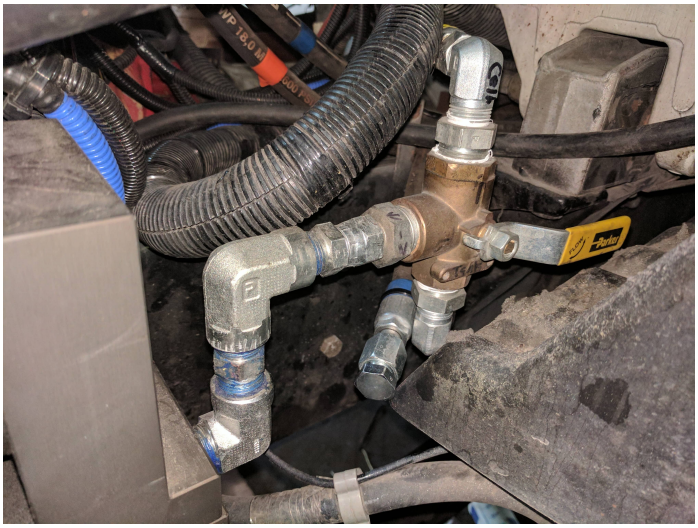

Figure 2.11. Suction valve - Only one fuel pipe connected.

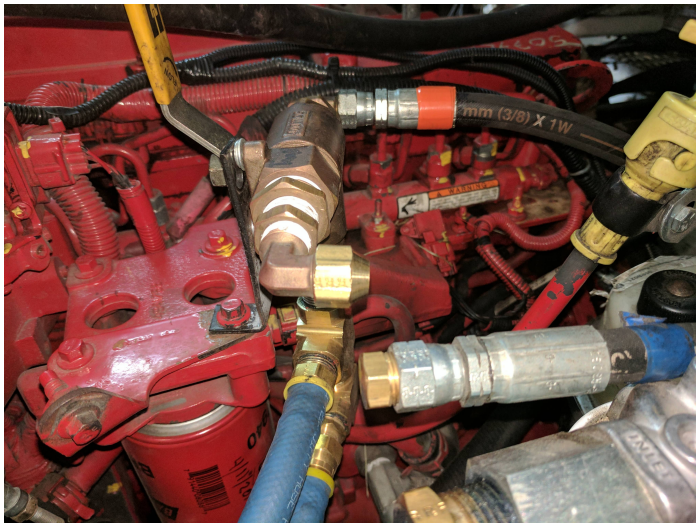

Figure 2.12. Return valve - Only one fuel pipe connected.

After making sure that the fuel can be used only from one tank, the next step in the process of getting ready for testing the truck on road is to refill the test tank with diesel and install it in the prototype tractor. The fuel tank is transported to a nearby gas station on a pick-up truck and filled with a total of 66.005 gallons of fuel.

Once the tank is filled with required amount of fuel, it is taken back and weighed using the same weighing scale, as shown in Figure 2.13 . As seen from Figure 2.14, the weight of the filled fuel tank is measured to be 566.6 lbs.

After the weight of the filled fuel tank is measured, the tank is installed in the tractor and necessary plumbing connections are made. This process includes connecting the suction line and the return line from the engine to the suction valve and return valve of the fuel tank. The pipe with yellow band, connecting to the left valve of the tank indicates the suction line of the engine and the one with orange band, connecting to the right valve of the tank indicates the return line for the engine. A picture of the tank after it's installed in the tractor is shown in Figure 2.15. This completes the calibration and installation procedure of the fuel tank before the on-road testing, which is described in the next section.

Figure 2.13. Weighing the filled fuel tank.

Figure 2.14. Weight of the filled fuel tank, wooden pallet.

2.1.2 On-road Testing of the Truck

The prototype truck was tested on-road on 27 June, 2017, the day following the calibration and installation of the fuel tank. The testing process for this particular test started around 4:00 AM and ended around 1:00 PM.

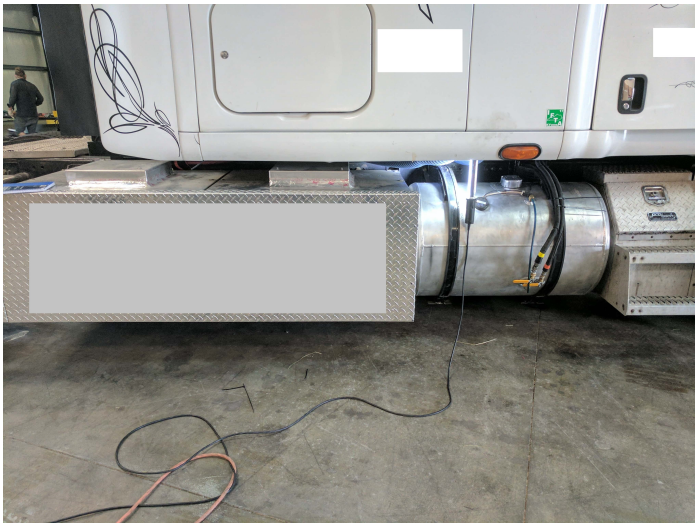

Figure 2.15. Filled fuel tank after connecting to the tractor.

The first step before performing the on-road test is to couple the tractor to the trailer. A picture taken while coupling the trailer and tractor is shown in Figure 2.16. Since the information associated with the test, such as speed, and number of miles traveled during the test are required to be recorded in order to calculate fuel economy, the GPS recording device along with the odometer are reset after the trailer and tractor are coupled.

The odometer reading after resetting the odometer is shown in Figure 2.17. The reading on top shows the cumulative number of miles while the reading on bottom shows the number of miles driven after resetting the odometer. As seen from the picture, the cumulative number of miles at the beginning of the test are recorded to be 27991 miles.

Once the tractor and trailer are coupled and GPS, odometer reset, the on-road testing of truck begins. Figure 2.18 shows a picture of the truck during the on-road test. The destination of the to-trip is Cambridge, Ohio. A photo of the truck after reaching the destination is shown in Figure 2.19. After a short break at the destination, return trip to Florence, Kentucky starts and Figure 2.20 shows a photo of the truck while on the return trip to Florence, Kentucky.

Figure 2.16. Connecting the tractor to the trailer.

Figure 2.17. Reading of odometer before the test.

Figure 2.18. A photo taken during to-trip.

Figure 2.19. Destination of to-trip.

Figure 2.20. A photo taken during return-trip.

After returning to the start-up, which is shown in Figure 2.21, the odometer reading is recorded once again in order to calculate the number of miles driven during the particular test. This reading is shown in Figure 2.22 and the cumulative number of miles after the test is completed are recorded as 28397 miles and the total number of miles traveled during the test are recorded as 405.6 miles.

Figure 2.21. End of test.

Figure 2.22. Odometer reading after test.

After the odometer reading is recorded, the tractor is decoupled from the trailer (see Figure 2.23) and only the tractor is driven inside the yard in order to measure the weight of the fuel tank after the test. The fuel tank is then disassembled from the tractor and carried to the weighing scale using a forklift and it's weight is measured.

This is shown in Figure 2.24. As seen from the figure, the weight of the fuel tank after the test is measured to be 165.2 lbs.

Figure 2.23. Prototype tractor after uncoupling from trailer.

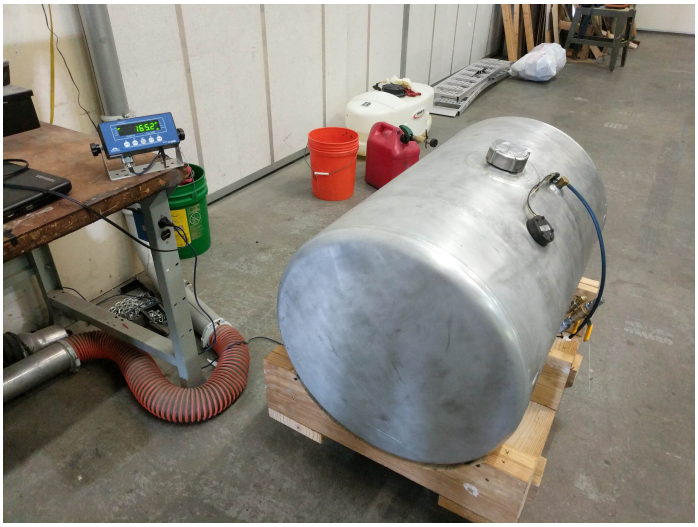

Figure 2.24. Weight of fuel tank after test.

2.1.3 Fuel Economy Calculations

Weight of tank, pallet + residual in-tank fuel before refill = 105.8 lb

Weight of tank + pallet after refuelling the tank = 566.6 lb

Weight of tank, pallet + remaining fuel after the test = 165.2 lb

Weight of fuel used during the test = 566.6 lb - 165.2 lb = 401.4 lb or 182.7 kg

Number of miles driven during the test = 405.6 miles

Fuel economy for the test (miles/kg) = $\frac{405.6 \text{ miles}}{182.07 \text{ kg}}$ = 2.228 miles per kg

Since there is no information about initial and final SOC of the battery, there is some degree of uncertainty introduced while calculating the fuel economy. The best case scenario for fuel economy will be when the battery pack starts at a state of charge of 100% and ends at a state of charge of 0%. Similarly, the worst case scenario will be when the battery pack starts at a state of charge of 0% and ends at a state of charge of 100%. Therefore, it would be more accurate to indicate a range of fuel consumption by taking into account the effect of this uncertainty, as indicated below.

Number of cells in series = 46

Energy capacity of each cell = 558 Wh

Total energy capacity of the battery pack = 46 $\times$ 558 Wh = 25668 Wh

Lower heating value (LHV) of diesel = 42.78 MJ/kg = 11883.33 Wh/kg

Assuming an average efficiency of 40% for the engine, the amount of diesel in kg that is required to charge the battery pack from 0% SOC to 100% SOC is

$$\frac{\text{Energy capacity of battery pack}}{\text{LHV of diesel} \times \text{ Efficiency of the engine}} = \frac{25668 \text{ Wh}}{11883.33 \text{ Wh/kg} \times 0.4} = 5.40 \text{ kg}$$

The estimated cumulative fuel consumption = 182.07 $\pm$ 5.40 kg = 404.40 $\pm$ 11.91 lb

The estimated fuel economy (miles/kg) = $\frac{405.6 \text{ miles}}{182.07 \pm 5.40 \text{ kg}}$ = 2.164 to 2.296 miles/kg

2.2 Summary of all Tests

This section summarizes the fuel economy results of all the tests performed during this phase. Table 2.2 lists the results of all tests, including the test date, gross vehicle weight, cruising speed and fuel economy. The 'min' and 'max' values of fuel economy for all tests are calculated taking into account the effect of uncertainty due to SOC of battery, as mentioned before. 'To' indicates To-trip and 'Re' indicates Return trip. The gross vehicle weight of the truck varies between To and Return trips in tests 3-9 as the same cargo is not transported back to the starting point (Florence, Kentucky).

Table 2.2. Summary of all tests performed.

Test #	Test Date	Tractor Weight	Trailer Weight	Trailer Cargo Weight	Gross Vehicle Weight	Average Cruise Speed	Estimated Fuel Economy	
		lb	lb	lb	lb	mph	mi per kg	km per kg
1	06/27/2017	22,400	Trailer + Cargo: 31,860		54,260	To: 55.0 Re: 55.0	min: 2.164 max: 2.296	min: 3.483 max: 3.695
2	08/01/2017	22,400	Trailer + Cargo: 31,860		54,260	To: 55.0 Re: 55.0	min: 2.143 max: 2.272	min: 3.449 max: 3.656
3	09/13/2017	17,599	19,000	To: 15,953.43 Re: 20,863.75	To: 52,552.43 Re: 57,462.75	To: 64.8 Re: 63.7	1.717	2.763
4	09/30/2017	22,400	19,000	To: 17,150.44 Re: 15,760.89	To: 58,550.44 Re: 57,160.89	To: - Re: -	min: 2.058 max: 2.174	min: 3.312 max: 3.499
5	10/18/2017	22,400	19,000	To: 17,094.73 Re: 18,987.34	To: 58,494.73 Re: 60,387.34	To: - Re: -	min: 2.051 max: 2.165	min: 3.301 max: 3.484
6	10/31/2017	22,400	19,000	To: 19,629.05 Re: 10,462.97	To: 61,029.05 Re: 51,862.97	To: - Re: -	min: 1.981 max: 2.088	min: 3.188 max: 3.360
7	11/02/2017	22,400	19,000	To: 24,080.89 Re: 17,636.55	To: 65,480.89 Re: 59,036.55	To:- Re: -	min: 2.029 max: 2.142	min: 3.265 max: 3.447
8	11/08/2017	22,400	19,000	To: 18,566.64 Re: 13,993.64	To: 59,966.64 Re: 55,393.64	To: - Re: -	min: 2.036 max: 2.149	min: 3.277 max: 3.458
9*	11/16/2017	22,400	19,000	To: 21,291.73 Re: 13,952.02	To: 62,709.73 Re: 55,352.02	To: - Re: -	min: 2.012 max: 2.172	min: 3.238 max: 3.495
10	11/29/2017	22400	Trailer + Cargo: 58,960		58,960	To: 55.0 Re: 55.0	min: 2.339 max: 2.493	min: 3.764 max: 4.012

*For test 9, fuel economy for only the To part of the trip was calculated as there was a mechanical coupler failure during the return trip. Therefore the test had to be stopped at that point and the truck was towed back.

It should be noted that the only test where both driver/tractor combination of package delivery/package delivery is present is the 09/13/17 test, which is test #3. In every other test, the tractor used is the one designed by the start-up and has a hybrid

powertrain. Figure 2.25 shows the fuel economy of each test performed in miles/kg, without considering the uncertainty due to SOC of battery. It can be observed that test performed with a package delivery tractor/package delivery driver combination has a considerably lower fuel economy as compared to other tests. This is due to the fact that the truck had a cruising speed of 65 mph while in the other tests, it was around 55 or 60 mph. Also, the tests performed with the prototype tractor/Package delivery driver combination have a lower fuel economy than the tests performed with a prototype tractor/start-up driver combination. This difference is due to both a variance in driving styles and also the GVW of the truck. The tests performed with a prototype tractor/start-up driver combination have a cruising speed of 55 mph while the ones with prototype tractor/package deliver driver combination do not have a cruising speed. The speed profiles for all these tests is shown in the next section.

2.2.1 Speed Profiles of all Tests Performed

Using the GPS recorded information obtained during testing, the speed profiles of every test performed are shown in Figures 2.26 - 2.35. Figures 2.26, 2.27, 2.35 represent the truck speed profiles during tests performed with prototype tractor/start-up driver combination. Figure 2.28 shows the speed profile of the test performed with a package delivery tractor/package delivery driver combination. Figures 2.29 - 2.34 show the speed profiles of tests performed with a prototype tractor/package delivery driver combination. The gaps in the speed profiles indicate a period of time during which the truck was stopped, either at a rest area or because of a problem in the truck. In an ideal scenario, there wouldn't be any stops during freight transportation over this tested route.

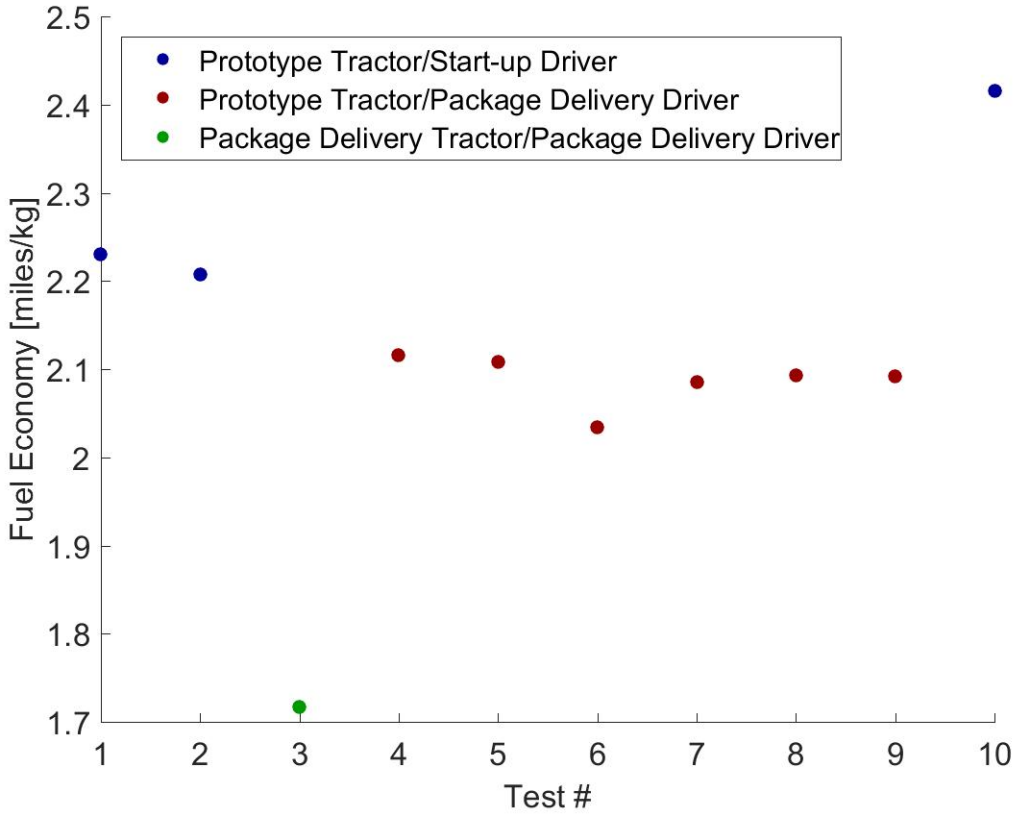

Figure 2.25. Fuel economy distribution.

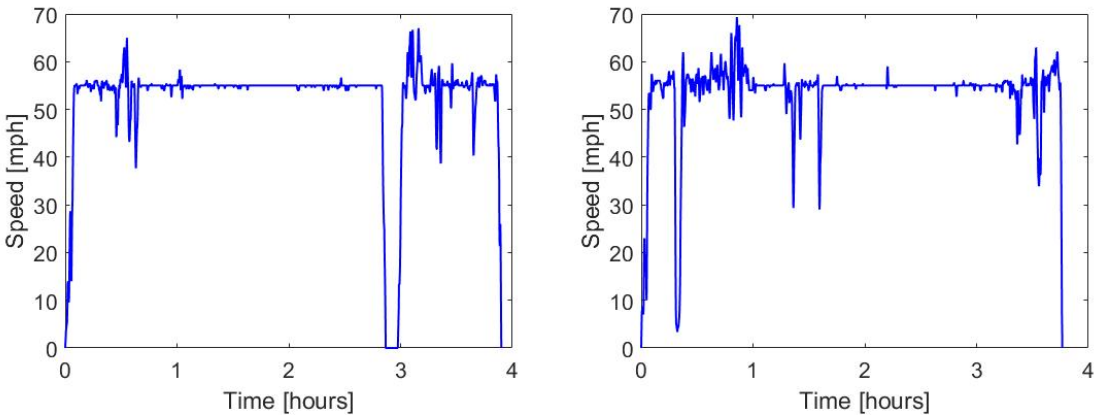

(a) (b)

Figure 2.26. Speed profile for 06/27/17 test (a) To route (b) Return route.

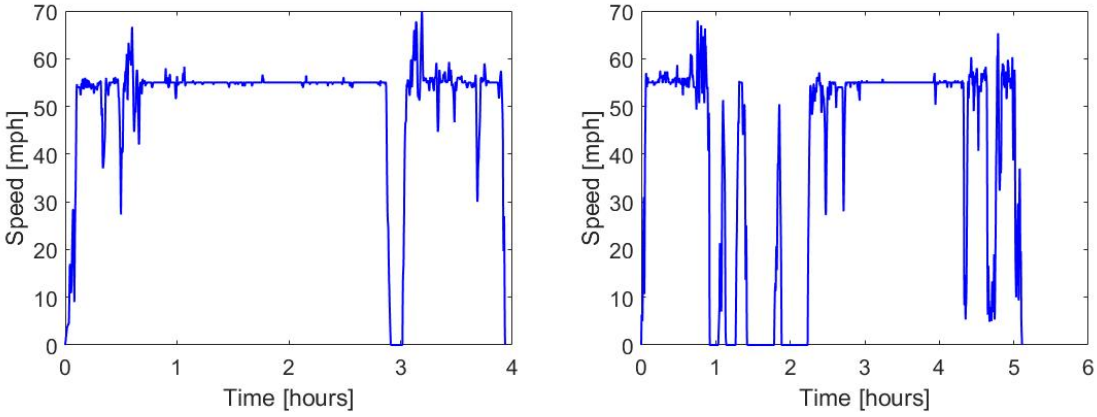

(a) To (b) Return

Figure 2.27. Speed profile for 08/01/17 test (a) To route (b) Return route.

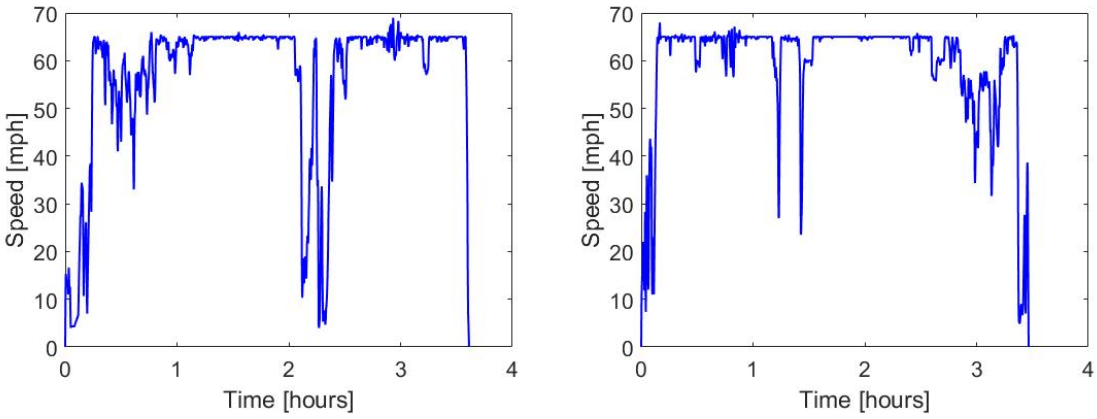

(a) To (b) Return

Figure 2.28. Speed profile for 09/13/17 test (a) To route (b) Return route.

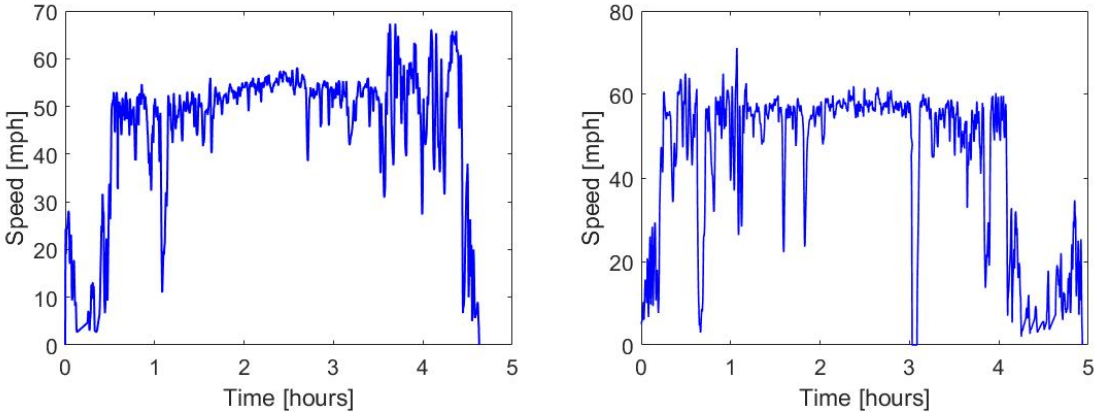

(a) To (b) Return

Figure 2.29. Speed profile for 09/30/17 test (a) To route (b) Return route.

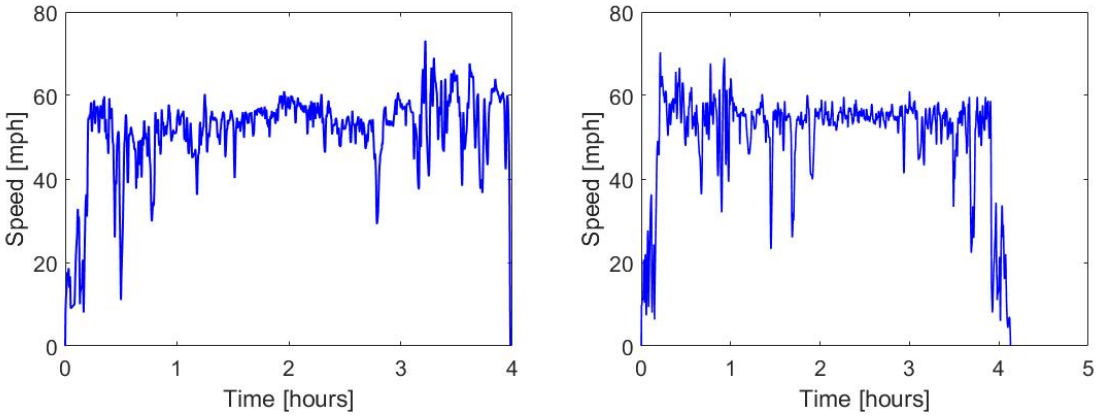

(a) To (b) Return

Figure 2.30. Speed profile for 10/18/17 test (a) To route (b) Return route.

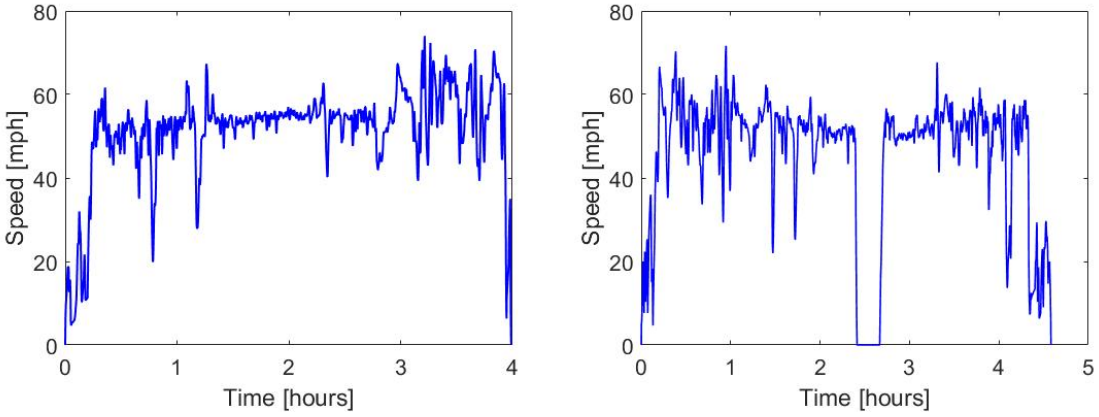

(a) To (b) Return

Figure 2.31. Speed profile for 10/31/17 test (a) To route (b) Return route.

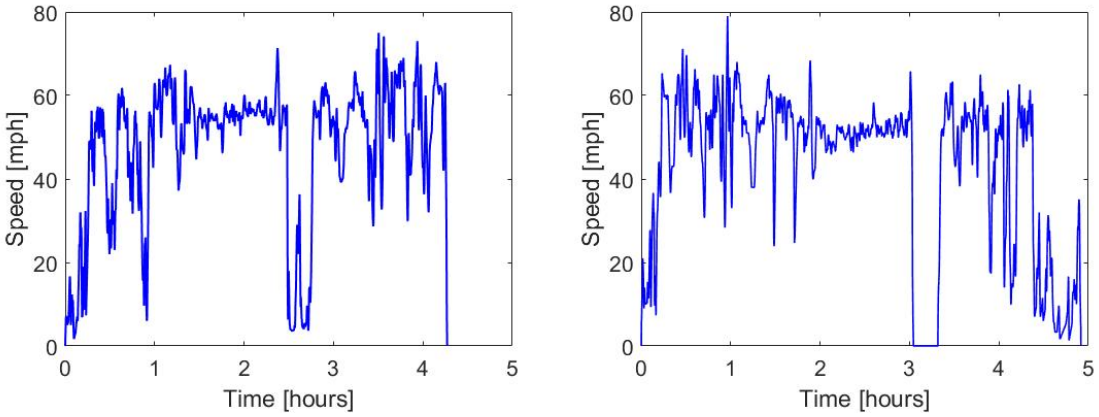

(a) To (b) Return

Figure 2.32. Speed profile for 11/02/17 test (a) To route (b) Return route.

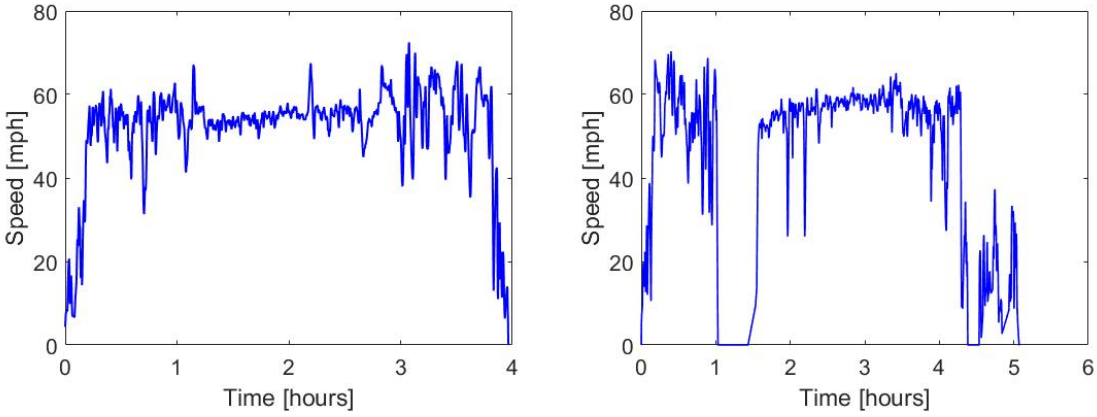

(a) To (b) Return

Figure 2.33. Speed profile for 11/08/17 test (a) To route (b) Return route.

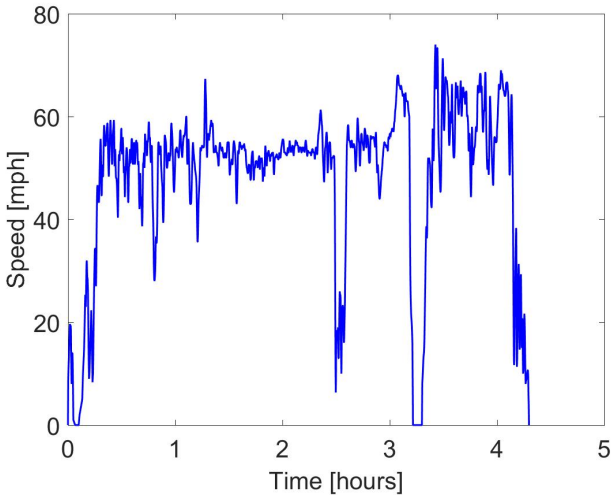

Figure 2.34. Speed profile for to-trip for 11/16/17 test.

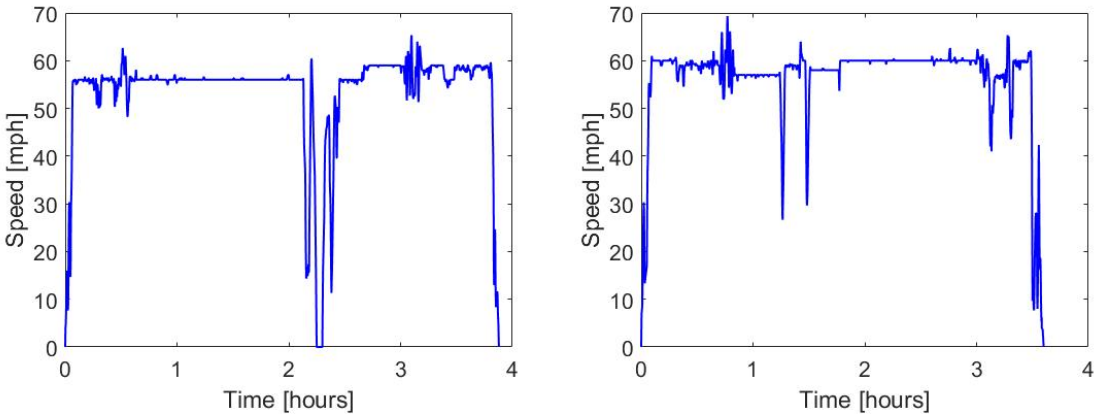

(a) To (b) Return

Figure 2.35. Speed profile for 11/29/17 test (a) To route (b) Return route.

2.2.2 Statistics of Fuel Economy

5/01/17
9:34:25

FUEL TAX DEDUCTION SHEETSHEETS
REPORT FOR 01/01/2017 THROUGH 03/31/2017

PITT5
PTX950RL
PAGE: 31

CONTRACT/ISP NAME	REPORT QTR	CONTRACT/ISP	PSAID	STTN NO.
NKY EXPRESS, INC	FIRST	C7580004	123459	0406

TRACTOR	STATE	TOTAL MILES	TOLL MILES		NET MILES	MPG		GALLONS USED	RATE ON TAX RETURN: TAX RATE	TAX PAID	RATE AT PUMP: GALLONS PURCHASED		TAX RATE	PURCHASED CREDIT	AMOUNT DUE	CREDIT AMOUNT
129263	KY	1,855.0	.0		1,855.0	7.17	=	258.7X	.3180	82.27	377.7	X	.2160	81.58	.69	
129263	NJ	357.0	.0		357.0	7.17	=	49.8X	.3340	16.63	261.6	X	.3340	87.37		70.74
129263	OH	1,190.0	.0		1,190.0	7.17	=	166.0X	.2800	46.47	.0	X	.2800	.00	46.47	
129263	PA	1,967.0	.0		1,967.0	7.17	=	274.3X	.7470	204.92	.0	X	.7470	.00	204.92	
129263	TN	282.0	.0		282.0	7.17	=	39.3X	.1700	6.69	158.7	X	.1700	26.98		20.29
129263	WV	78.0	.0		78.0	7.17	=	10.9X	.3220	3.50	.0	X	.3220	.00	3.50	
SUBTOTAL:		5,729.0	.0		5,729.0			799.0		360.48	798.0			195.93	255.58	91.03
														AMOUNT DUE	164.55	
129279	KY	3,488.0	.0		3,488.0	5.31	=	656.9X	.3180	208.88	4829.0	X	.2160	1043.06		834.18
129279	OH	20,881.0	.0		20,881.0	5.31	=	3,932.4X	.2800	1,101.07	.0	X	.2800	.00	1,101.07	
129279	TN	414.0	.0		414.0	5.31	=	78.0X	.1700	13.25	.0	X	.1700	.00	13.25	
129279	WV	884.0	.0		884.0	5.31	=	166.5X	.3220	53.60	.0	X	.3220	.00	53.60	
SUBTOTAL:		25,667.0	.0		25,667.0			4,833.8		1,376.80	4,829.0			1,043.06	1,167.92	834.18
														AMOUNT DUE	333.74	
130188	KY	1,557.0	.0		1,557.0	5.26	=	296.0X	.3180	94.13	3680.4	X	.2160	794.97		700.84
130188	OH	17,287.0	.0		17,287.0	5.26	=	3,286.5X	.2800	920.22	.0	X	.2800	.00	920.22	
130188	PA	517.0	.0		517.0	5.26	=	98.3X	.7470	73.42	.0	X	.7470	.00	73.42	
130188	WV	28.0	.0		28.0	5.26	=	5.3X	.3220	1.71	.0	X	.3220	.00	1.71	
SUBTOTAL:		19,389.0	.0		19,389.0			3,686.1		1,089.48	3,680.4			794.97	995.35	700.84
														AMOUNT DUE	294.51	
136522	KY	1,534.0	.0		1,534.0	6.00	=	255.7X	.3180	81.30	1285.7	X	.2160	277.71		196.41
136522	NJ	2,163.0	.0		2,163.0	6.00	=	360.5X	.3340	120.41	3037.8	X	.3340	1014.63		894.22
136522	OH	9,119.0	.0		9,119.0	6.00	=	1,519.8X	.2800	425.55	.0	X	.2800	.00	425.55	
136522	PA	12,550.0	.0		12,550.0	6.00	=	2,091.7X	.7470	1,562.47	.0	X	.7470	.00	1,562.47	
136522	TN	72.0	.0		72.0	6.00	=	12.0X	.1700	2.04	.0	X	.1700	.00	2.04	
136522	WV	537.0	.0		537.0	6.00	=	89.5X	.3220	28.82	.0	X	.3220	.00	28.82	
SUBTOTAL:		25,975.0	.0		25,975.0			4,329.2		2,220.59	4,323.5			1,292.34	2,018.88	1,090.63
														AMOUNT DUE	928.25	
136550	IN	368.0	.0		368.0	5.03	=	73.2X	.2700	19.75	.0	X	.1600	.00	19.75	
136550	KY	25,205.0	.0		25,205.0	5.03	=	5,010.9X	.3180	1,593.48	1421.6	X	.2160	307.07	1,286.41	
136550	OH	149.0	.0		149.0	5.03	=	29.6X	.2800	8.29	.0	X	.2800	.00	8.29	
136550	TN	3,954.0	.0		3,954.0	5.03	=	786.1X	.1700	133.63	4470.0	X	.1700	759.90		626.27
SUBTOTAL:		29,676.0	.0		29,676.0			5,899.8		1,755.15	5,891.6			1,066.97	1,314.45	626.27

Figure 2.36. IFTA form for the conventional package delivery truck on this route.

Table 2.3. Statistics of estimated fuel economy.

Estimated Fuel Economy	Start-up driver Test: 1,2,10		Package delivery driver Test: 4,5,6,7,8,9		All tests Test:1,2,4,5,6,7,8,9,10	
	mi per kg	km per kg	mi per kg	km per kg	mi per kg	km per kg
Average value	min: 2.215 max: 2.354	min: 3.565 max: 3.788	min: 2.028 max: 2.148	min: 3.264 max: 3.457	min: 2.090 max: 2.217	min: 3.364 max: 3.567
Median value	min: 2.164 max: 2.296	min: 3.483 max: 3.695	min: 2.033 max: 2.157	min: 3.271 max: 3.471	min: 2.051 max: 2.172	min: 3.301 max: 3.495

Based on the International Fuel Tax Agreement (IFTA) form (Figure 2.36) provided by the start-up, the fuel economy of the conventional tractor over the Cambridge route from 1 January, 2017 to 31 March, 2017 was $\frac{5.260 \text{ miles/gal}}{3.149 \text{ kg/gal}} = 1.670$ miles per kg (assuming density of diesel to be 0.832 kg/l). Table 2.3 shows the average and median values of estimated fuel economy of tests with the prototype tractor.

3. MODELING OF THE PROTOTYPE TRUCK AND SIMULATION

Although the real world testing of the prototype series electric hybrid truck provided information about fuel consumption, there is no means to calculate the fuel savings exclusively because of powertrain hybridization. This is due to the fact that there was not a test that was performed using a conventional truck on these same routes, with the same gross vehicle mass and similar speed profiles. In order to evaluate fuel savings due to powertrain electrification, a hybrid vehicle simulation can be compared to the fuel economy result with that of a conventional vehicle simulation on the same route to quantify the fuel savings.

This work also gives an opportunity to understand if there are any shortcomings of the current powertrain, or testing protocol and if there is any possibility of bettering the predicted fuel economy by modifying any powertrain parameters. This chapter describes the simulation model. The simulation is then performed on two different powertrain configurations, configuration that the prototype truck uses and an other configuration with a few modified powertrain parameters, which is described in detail later in the chapter.

3.1 Vehicle Simulation Model

A commercially available automotive simulation software named Autonomie, developed by Argonne National Labs, was used. It is a powerful and robust simulation tool for vehicle performance analysis. The software has a MATLAB/Simulink based environment and has all powertrain, driver, controller and environment component models defined. One of the benefits of using Autonomie is its flexibility to customize different parameters, architectures, models etc. with high ease.

The powertrain model that has been used for the simulation in this project is a series hybrid electric architecture based on the prototype powertrain. Figure 3.1 shows a series HEV powertrain modeled in Autonomie. The ICE is connected in series with the Energy Storage System (ESS) and if possible and needed, the engine has a capability to charge the battery through the generator. The required tractive power at wheels is directly provided by the electric motor.

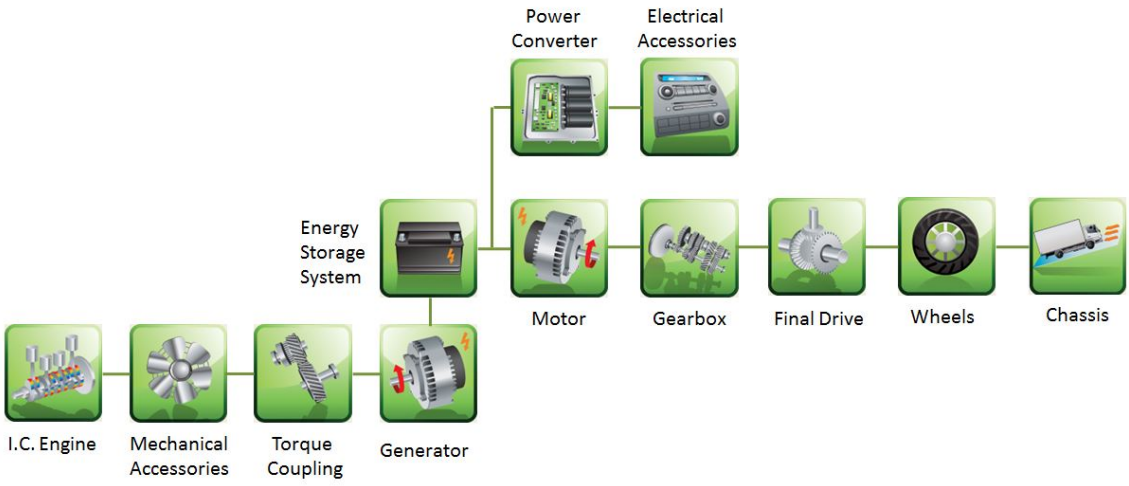

Figure 3.1. Series hybrid electric vehicle powertrain architecture.

The full vehicle model, developed in Autonomie, broadly has three components

- Driver
- Vehicle Powertrain Controller (vpc)
- Vehicle Powertrain Architecture (vpa)

The input to the vehicle model is the desired drive cycle, which includes both the desired speed and the desired grade. The model then predicts the behavior of all components in the vehicle. The driver model is a forward facing (look-ahead) model and it accepts the desired drive cycle as the input, calculates the desired accelerator and brake pedal positions at every instant of time. These accelerator and brake pedal positions are computed based on the required instantaneous torque needed to propel

the vehicle at that particular speed while being able to meet the grade requirement. The torque required is determined from the tractive force required to generate required acceleration at the wheels while overcoming the rolling resistance, resistance due to aerodynamic drag and resistance due to grade. The equation that represents tractive force required at the wheels at any instant of time is shown below in Equation (3.1).

$$F_{tractive} = M\frac{dv}{dt} + MgC_{rr} + \frac{1}{2}C_D\rho Av^2 + Mgsin\theta \tag{3.1}$$

where:

M : Vehicle mass

v : Vehicle speed

g : Acceleration due to gracity

C_{rr} : Coefficient of rolling resistance

C_D : Coefficient of aerodynamic drag

ρ : Density of air

A : Frontal area of the vehicle

θ : Road grade

Based on the accelerator and brake pedal positions that are output by driver, which are inputs to vpc, it calculates engine power, battery power required among other things based on the energy management strategy that is being used. This power split between engine and battery is determined while also taking care of the physical constraints of powertrain models. These constraints include instantaneous torque, power limits of engine, generator, and motor as well as charging and discharging power limits for the battery.

The maximum torque that the engine, generator, motor can provide is dependent on the speed of operation, as shown in Equations (3.2) - (3.4) . Also, the efficiency of operation of each of these powertrain components is a function of their angular speed as well as torque that is being generated (Equations (3.5) - (3.7)). The power that the battery can dissipate while discharging as well as the power that it can accept

while charging is a function of the state of charge of the battery (Equations (3.8) , (3.9). These relationships are modeled using 1-D, 2-D look-up maps in Autonomie.

$$T_{max,eng} = f(N_{eng}) \tag{3.2}$$

$$T_{max,gen} = f(N_{gen}) \tag{3.3}$$

$$T_{max,mot} = f(N_{mot}) \tag{3.4}$$

$$\eta_{eng} = f(N_{eng}, T_{eng}) \tag{3.5}$$

$$\eta_{gen} = f(N_{gen}, T_{gen}) \tag{3.6}$$

$$\eta_{mot} = f(N_{mot}, T_{mot}) \tag{3.7}$$

$$P_{max(discharge),batt} = f(SOC) \tag{3.8}$$

$$P_{max(charge),batt} = f(SOC) \tag{3.9}$$

where T_{max} is maximum torque, N is angular speed, η is efficiency, T is torque, P represents power and $eng, gen, mot, batt$ represent ICE, generator, motor and battery, respectively.

3.2 Powertrain Model

The vehicle powertrain component models that are used for this simulation are shown in Table 3.1. Models of all these components are readily available in Autonomie but the generator model that is available in Autonomie has a peak power of only 160 kW. In order to tackle this issue, the generator power, torque, efficiency and speed maps are scaled up using a scaling parameter to match the required peak power rating of 261 kW.

The ESS is modeled as a series of 46 Nickel Metal Hydride (Ni-MH) cells, each with an energy capacity of 558 Wh and both mechanical and electrical accessory loads are modeled as constant power losses. The gearbox is modeled to be a 10 speed Eaton automatic transmission, the gear ratios varying from 10.96:1 to 0.74:1.

Table 3.1. Powertrain component models.

Powertrain Component	**Model**
Engine	Cummins ISB 6.7L Compression Ignition Engine
Generator	UQM Permanent Magnet Electric Generator
Motor	UQM Permananent Magnet Electric Motor
ESS	46 NiMH cells in series
Transmission	Eaton Ultra Shift 10 Speed RTO-16910

3.2.1 Battery Model

Existing battery models can be broadly divided into two kinds: electrochemical models and analytical-equivalent circuit models [10]. Electrochemical models use coupled nonlinear partial differential equations to exactly describe the chemical processes occurring inside a cell. Equivalent circuit models are computationally faster than electrochemical models and are modeled as a circuit in which the internal impedance is a combination of chemical reactions, resistance of electrodes, etc. It is typically modeled as a resistance in series with zero or more resistance-capacitance branches. For this simulation, the battery is modeled using an equivalent circuit model.

Figures 3.2 and 3.3 show zero and first order equivalent circuit representations of a cell, respectively. For this study, a zero order battery model has been used.

In the circuit shown in Figure 3.2, E_0 represents the open circuit voltage of the battery and it is the voltage that the battery exhibits when there is no load attached to the cell. This open-circuit voltage is a function of SOC of the battery. R_0 represents an ohmic resistance that accounts for resistances of cell connectors, cathode and anode, etc. V_{batt} represents the actual voltage of the battery when there is a load attached to it and is called is the terminal voltage.

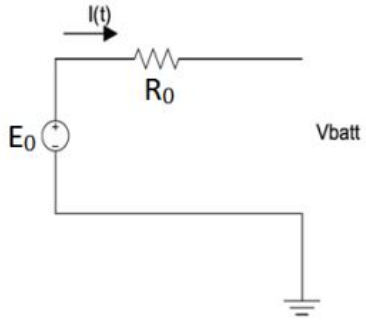

Figure 3.2. Zero order equivalent circuit representation of a cell.

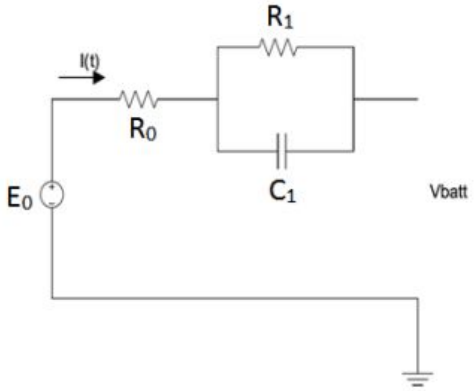

Figure 3.3. First order equivalent circuit representation of a cell.

For the first order model, similar to the zero order model, R_0 represents the resistances in connectors, electrodes while the R_1 C_1 branch models the drift and diffusion process of ions travelling through the electrolyte.

SOC of the battery is computed using Coulomb counting method, as shown in Equation (3.10). As mentioned earlier, this SOC is used to calculate the maximum power that the battery pack can provide during discharging/ charging. A plot that shows the physical charging/discharging constraints of the battery is shown in Figure 3.4.

$$SOC(t_2) = SOC(t_1) - \frac{\int_{t_1}^{t_2} idt}{Ah_{capacity}} \tag{3.10}$$

where i represents battery current and $Ah_{capacity}$ represents battery capacity in Ampere-hours

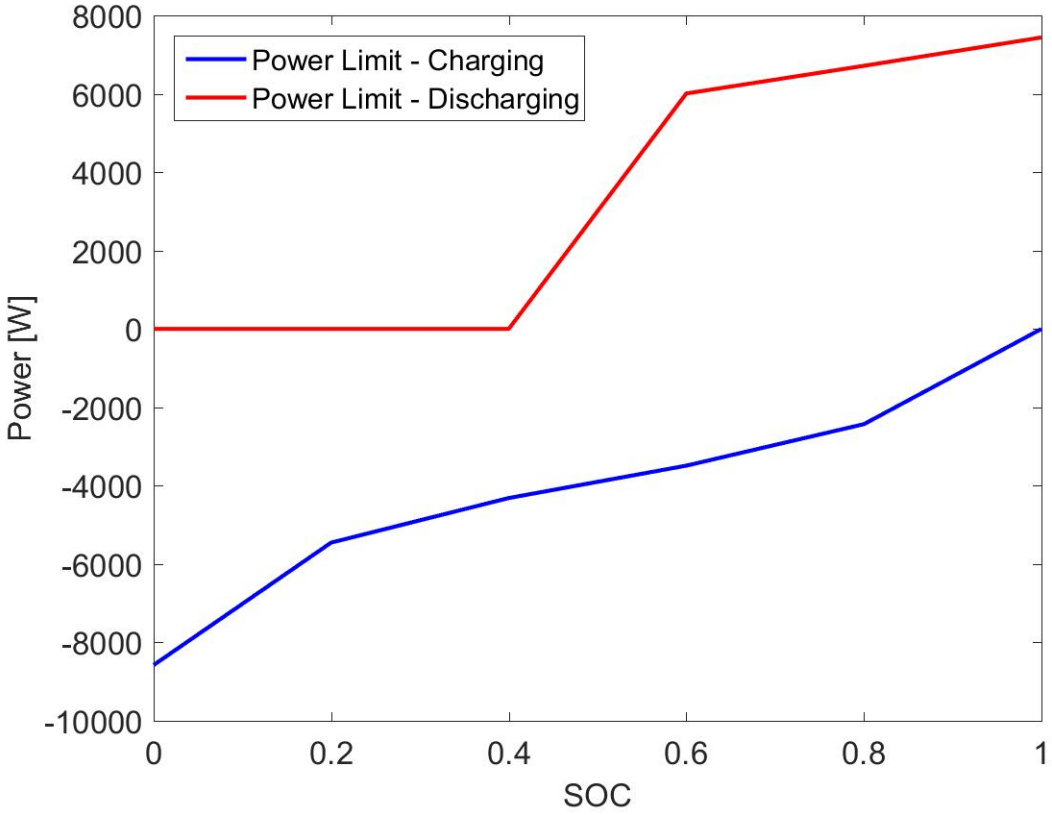

Figure 3.4. Cell power limits.

3.3 Energy Management Control Strategy

Any HEV can provide the required power at wheels through two sources of energy, the engine as well as the battery. This ability offers an opportunity to use two sources of power in a manner that has a potential to save fuel, if the components are sized optimally and if a relevant control strategy is being used. One of the key differences

between a HEV and PHEV is that the ESS in a PHEV can be recharged whenever needed, while one doesn't have such a choice when using a HEV. Therefore, any power management strategy that is designed for a HEV has two principal requirements:

- Split the required tractive power at the wheels into two parts, power that has to be supplied by the engine and the power that has to be supplied by the battery.
- Make sure that the SOC of the battery is maintained through out the use of the vehicle.

During braking, ESS of the vehicle can be recharged through regenerative braking and this is a significant factor in the ability to save fuel in a HEV. All the regenerative braking energy that is available when the vehicle is decelerating may not be captured by the battery as it is limited by both the electric machine as well as the power limit of battery during charging. During both acceleration and braking, the power management strategy has to determine how the required power should be split into two fractions in the most optimal manner, while not violating the imposed physical constraints on all the powertrain components.

For this project, a rule-based control strategy that is defined in Autonomie for a series electric hybrid vehicle has been used. Any HEV can be operated in two modes, namely EV only mode and HEV mode. EV mode refers to electric only mode where the engine is not used, which means the engine is set to OFF. This mode is typically used during very low power requirement scenarios (during vehicle starting). If this mode was not an option (like in a conventional vehicle), the engine would have been forced to operate at very low efficiency points. HEV mode refers to a scenario when the engine is in ON condition, that is, both the engine and battery are in operation. The power management strategy determines when the vehicle should be in EV or HEV mode based on the engine ON/OFF condition which depends on various factors. These conditions that demand the engine to be ON are listed below.

- If the current SOC of ESS is less than a predefined value of SOC at which the engine has to switch on, or

- If the power demand is greater than a fraction of the instantaneous discharge power limit of the battery (shown in Equation (3.11))

$$P_{demand} > X_{eng,ON} * P_{batt,max} \tag{3.11}$$

where, $X_{eng,ON}$ is a predefined fraction, P_{demand} is the instantaneous power required, $P_{batt,max}$ is the instantaneous maximum discharge power limit and it is a function of SOC, as mentioned earlier.

Once the engine is commanded to be ON, the vehicle in now in HEV mode. The engine power that is demanded by the power management strategy is calculated as the minimum of maximum engine power for that engine speed and the difference of power demanded at chassis and power demanded by ESS. This is shown in Equation (3.12).

$$P_{demanded,eng} = \min(P_{eng,max}, P_{demanded} - P_{demanded,batt}) \tag{3.12}$$

where $P_{demanded,eng}$ is the power that is demanded from the engine, $P_{eng,max}$ is the maximum power that the engine can supply, $P_{demanded}$ is the power that is being demanded by the chassis, $P_{demanded,batt}$ is the power that is demanded by ESS.

Since the power management strategy needs the ESS to maintain its SOC around the target SOC, it determines the power that is demanded by ESS based on the current SOC of ESS. When SOC is less than target SOC ($SOC < SOC_{Target}$), the battery power demand is a negative quantity, which means it needs to absorb power in order to maintain SOC. Usually, this is a scenario which happens when ESS provides power to assist the engine in propelling the vehicle which then leads to decrease in SOC to a point where it is less than target SOC. Similarly, when SOC is greater than target SOC ($SOC > SOC_{Target}$), the battery power demand is a positive quantity, which means it needs to discharge power in order to maintain SOC. SOC goes to a point that is greater than the target SOC when ESS has absorbed energy through absorption of

regenerative energy. As current SOC goes further away from target SOC, ESS needs to discharge more power for the SOC to be regulated. Similarly, when the current SOC less than the target SOC, ESS needs to discharge more power for the SOC to be regulated. This ESS power demand vs SOC (shown in Figure 3.5) is a simple look-up table that is built into the vehicle simulation model. Modifications can be made to this map depending on how strictly one wants to regulate the SOC. Changing the power demand curve so that it has higher slope represents strict regulation of SOC.

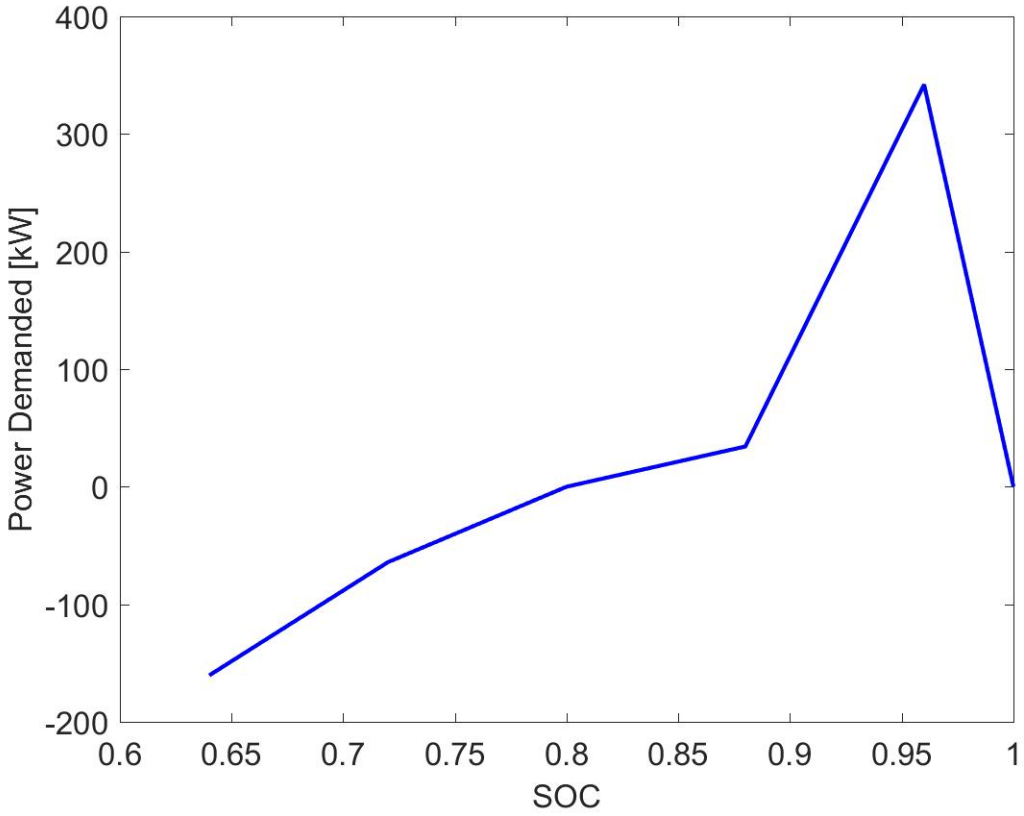

Figure 3.5. Battery power demanded based on current SOC.

3.4 Vehicle Parameters

Table 3.2 shows the list of vehicle parameters that have been used for simulating the prototype series electric hybrid truck.

Table 3.2. Vehicle parameters.

Parameter	Unit	Value
Powertrain Parameters		
Engine Peak Power	kW	261
Generator Peak Power	kW	261
Motor Peak Power	kW	150
Battery Energy Capacity	kWh	25.668
Torque Coupling	-	1
Final Drive Ratio	-	4:11
Power drawn by Mechanical Accessories	kW	26
Power drawn by Electrical Accessories	kW	5
Vehicle Characteristics		
Coefficient of Rolling Resistance (C_{rr})	-	$0.0012v + \min(0.04v, 0.002)$
Coefficient of Aerodynamic Drag (C_d)	-	0.6
Vehicle Mass	kg	Varying for each drive cycle
Vehicle Frontal Area	m^2	7.48

where v is the vehicle velocity

Even though the peak power of all powertrain components is exactly matching the ones during experimental testing, the models used for generator and motor in the simulation are not the same as the ones in the prototype powertrain because the data for these models is not available in Autonomie (The torque-speed maps for

generator and motor are not the same for every generator and motor with the same peak power).

3.5 Simulation Results

Using the information about the drive cycles that is obtained from real world testing of the truck, the vehicle simulation model that has been described earlier is simulated on three different drive cycles. The same powertrain architecture, i.e. a series electric hybrid architecture but with modified powertrain component sizes has also been simulated on these three drive cycles with an aim to decrease fuel consumption (increase fuel savings) and also meet the gradeability requirement, which is described later in the section. In order to quantify the fuel savings due to hybridization, the fuel consumption results obtained from this simulation are compared with the fuel consumption results obtained from simulating a conventional class 8 heavy-duty truck on the same routes.

As noticed from Figures 2.26 -2.35, there is a significant difference in speed profiles depending on the combination of tractor/trailer. As a reminder, in the tests performed with a combination of prototype tractor and start-up driver, the truck was mostly driven with cruise control around 55 mph. In the test performed with a combination of package delivery tractor and package delivery driver, the truck was driven with a speed around 65 mph. In the tests performed with a combination of a prototype tractor and package delivery driver, the truck was not driven using cruise control. Therefore, all these drive cycles were classified into three classes (Table 3.3), each representing one specific kind of drive cycle. For the simulation, one drive cycle from each of the three categories is selected and all vehicle models are simulated on each of these three drive cycles for comparison. Figures 3.6, 3.7 and 3.8 portray the drive cycles selected to represent category 1, 2 and 3, respectively.

Table 3.3. Categories of drive cycles.

Category	Driver	Tractor	Cruising Speed
1	Start-up	Prototype	55 mph
2	Package delivery	Prototype	No cruise control
3	Package delivery	Package delivery	65 mph

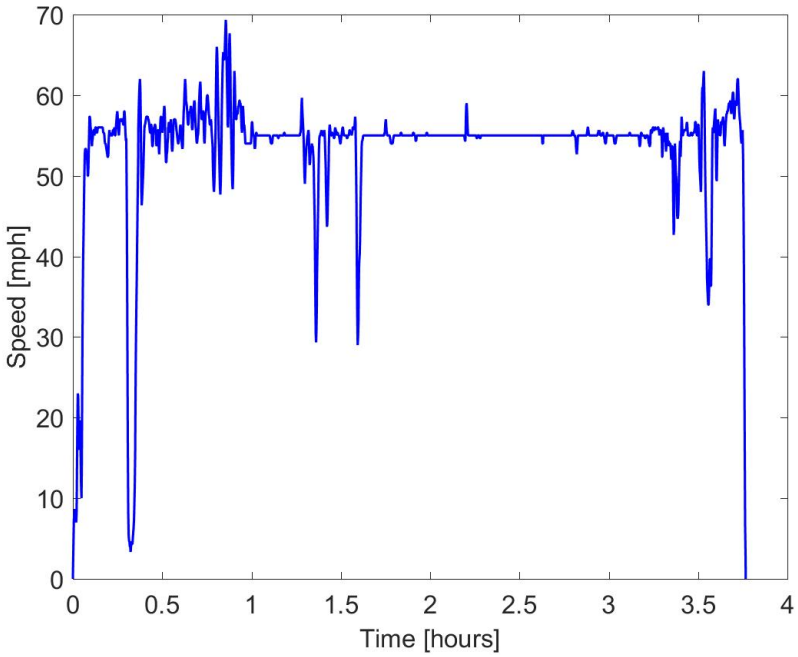

Figure 3.6. Drive cycle representing category 1.

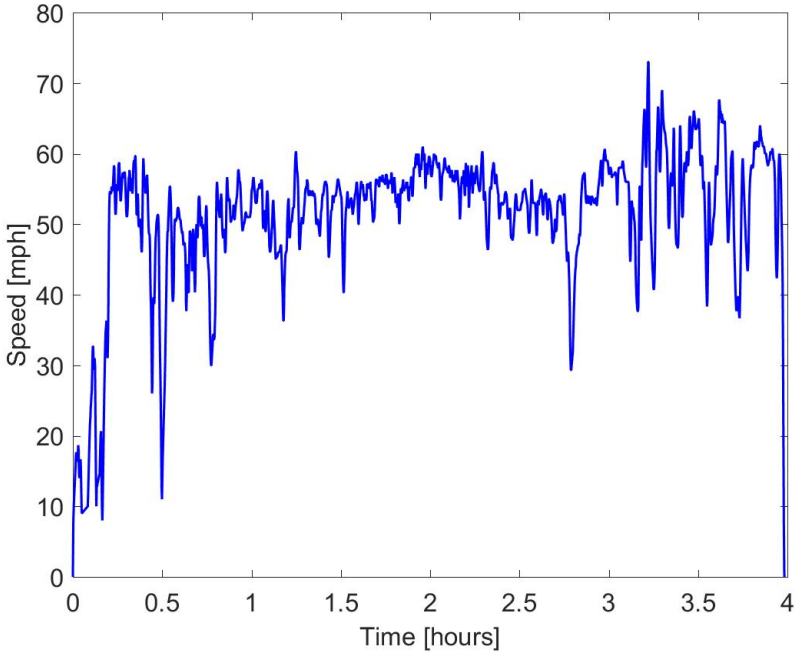

Figure 3.7. Drive cycle representing category 2.

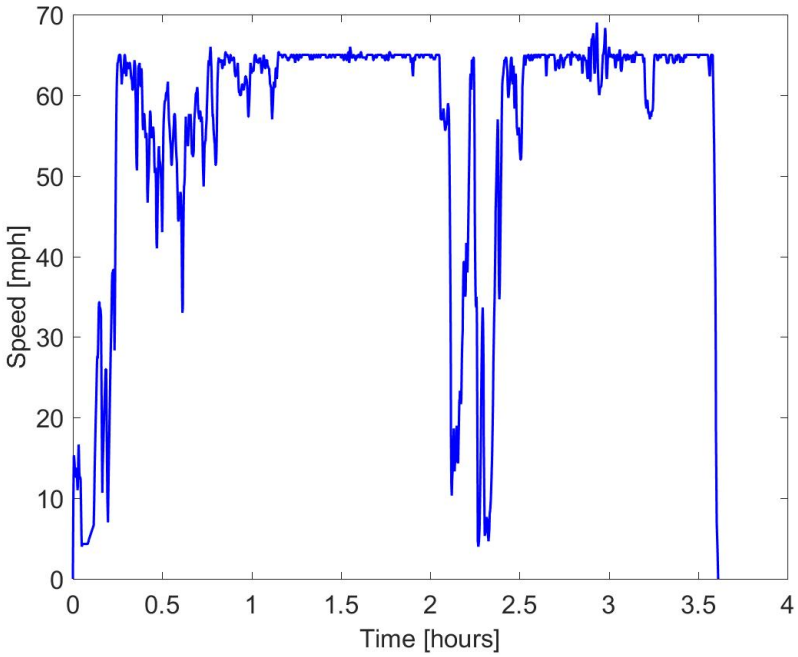

Figure 3.8. Drive cycle representing category 3.

3.5.1 Conventional Class 8 Heavy-Duty Truck Simulation - Baseline

The fuel economy of a conventional class 8 truck on these three routes is considered as the reference when calculating fuel savings due to hybridization. A powertrain model for a conventional heavy duty class 8 truck is available in Autonomie and the same model has been used for simulation. The fuel economy results on the three drive cycles that are under consideration are summarized in Table 3.4.

Table 3.4. Fuel economy of a conventional class 8 heavy-duty truck.

Drive Cycle	**Fuel Economy (mi/kg)**
1	2.07
2	2.06
3	1.73

It's seen that drive cycle 3 has considerably lower fuel economy when compared to drive cycles 1 and 2, which is an expected trend because the truck is consistently driven at 65 mph in drive cycle 3 when compared to 55 mph in drive cycle 1 and around 55-60 mph in drive cycle 2. The tractive power required at 65 mph would be significantly higher than that at 55-60 mph because of an increase in aerodynamic drag and rolling resistance, which are functions of vehicle velocity.

3.5.2 Engine Operating Range for Hybrid Powertrain

The engine operating speeds (shown in Figure 3.9) were obtained from a prior real world test conducted through the Engine Control Module (ECM). This shows that the engine is being operated between 1700 RPM and 1900 RPM. To replicate this, the same range of operating speeds is used for the engine in simulation also.

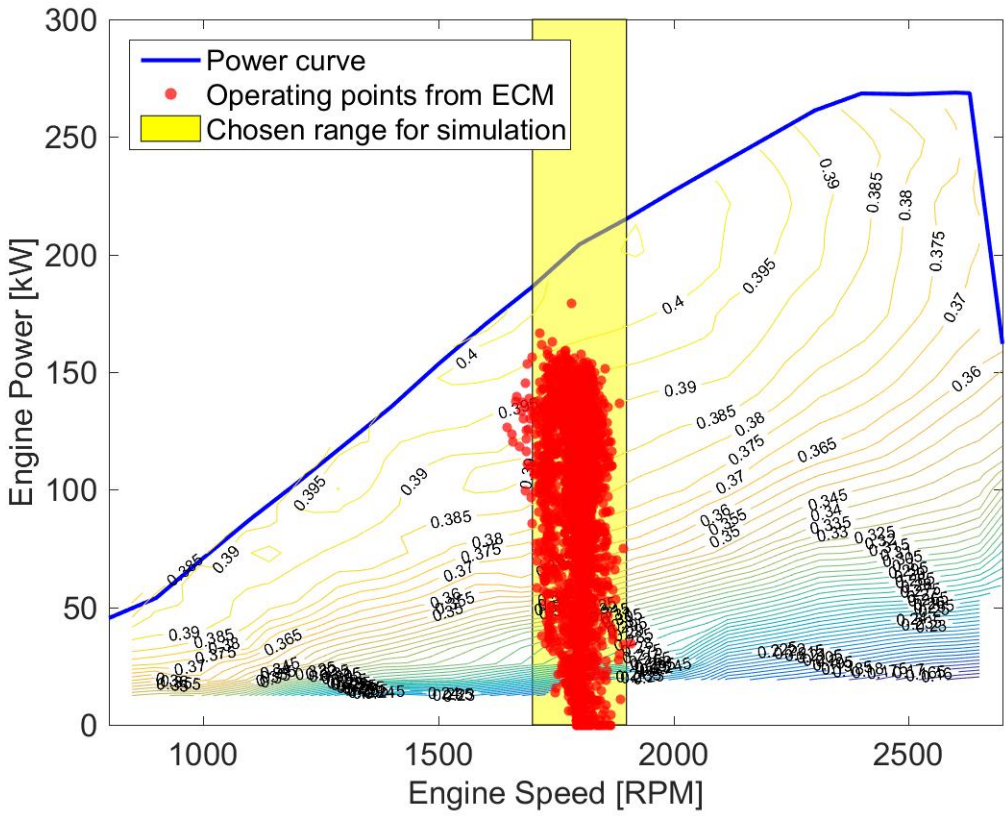

Figure 3.9. Operating range of engine.

3.5.3 Original Prototype Powertrain

This subsection describes the simulation results that have been obtained with the vehicle model described previously. In order to consider any vehicle simulation result to be acceptable, the simulation should satisfy these two criteria:

- The percentage of time for which the vehicle speed in the simulation is missing the drive cycle speed trace by more than 2 mph is less than 2 %.
- SOC of the battery is maintained through out the course of the drive cycle

As seen in Figure 3.10, the engine in hybrid powertrain in simulation is operating between 1700 RPM and 1900 RPM, as desired on all three drive cycles considered and is closely matching the speeds shown by ECM. Figure 3.11 shows a comparison

between the desired speed and actual speed of the truck and it can be noticed that there is rarely any period of time when simulated speed does not match the desired speed for all of the three drive cycles considered. Therefore, the trace requirement is met on all three drive cycles.

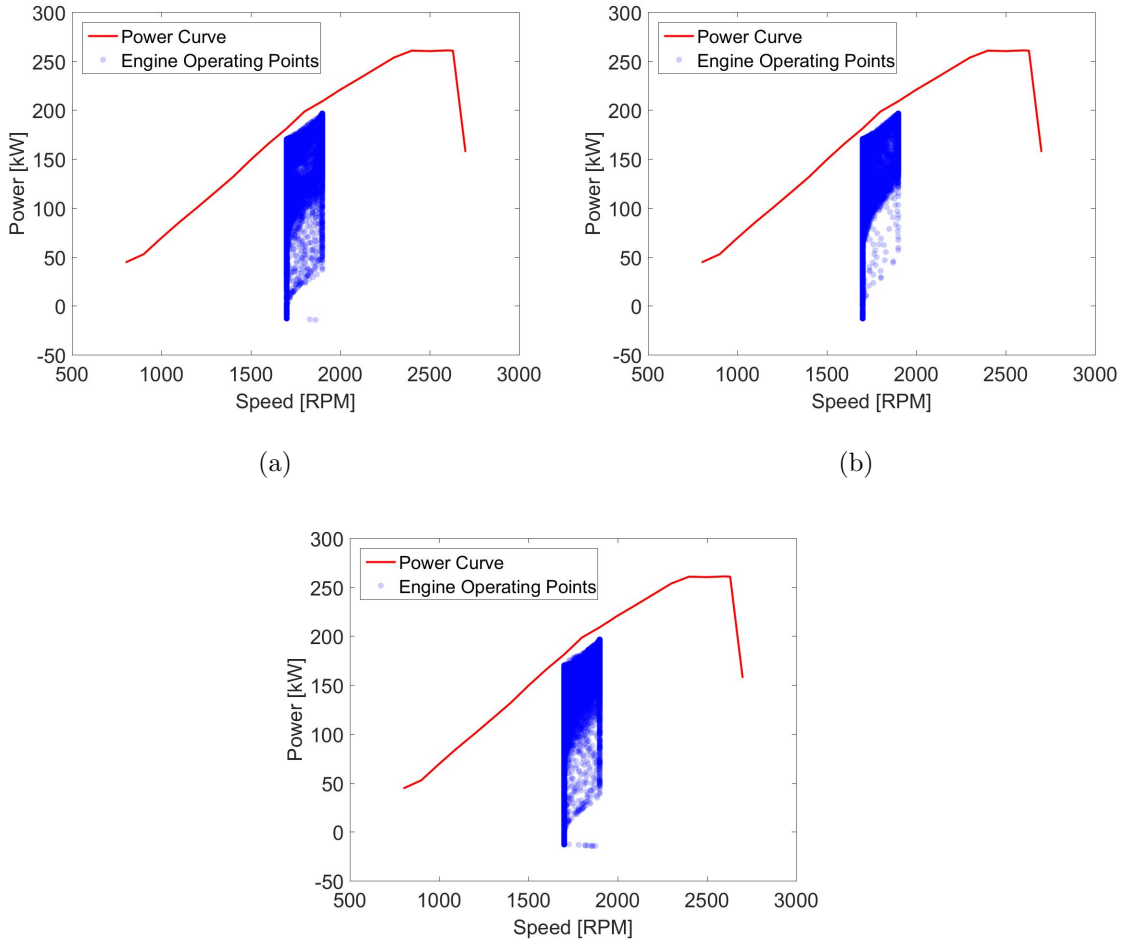

(a)

(b)

(c)

Figure 3.10. Engine operating points (a) Drive cycle 1 (b) Drive cycle 2 (c) Drive cycle 3.

It is observed from Figure 3.12 that SOC is always maintained around the target SOC (0.8) during all times and also the SOC at the end of simulation is very close to the target, for all of the three cases. Although there is a considerable range of

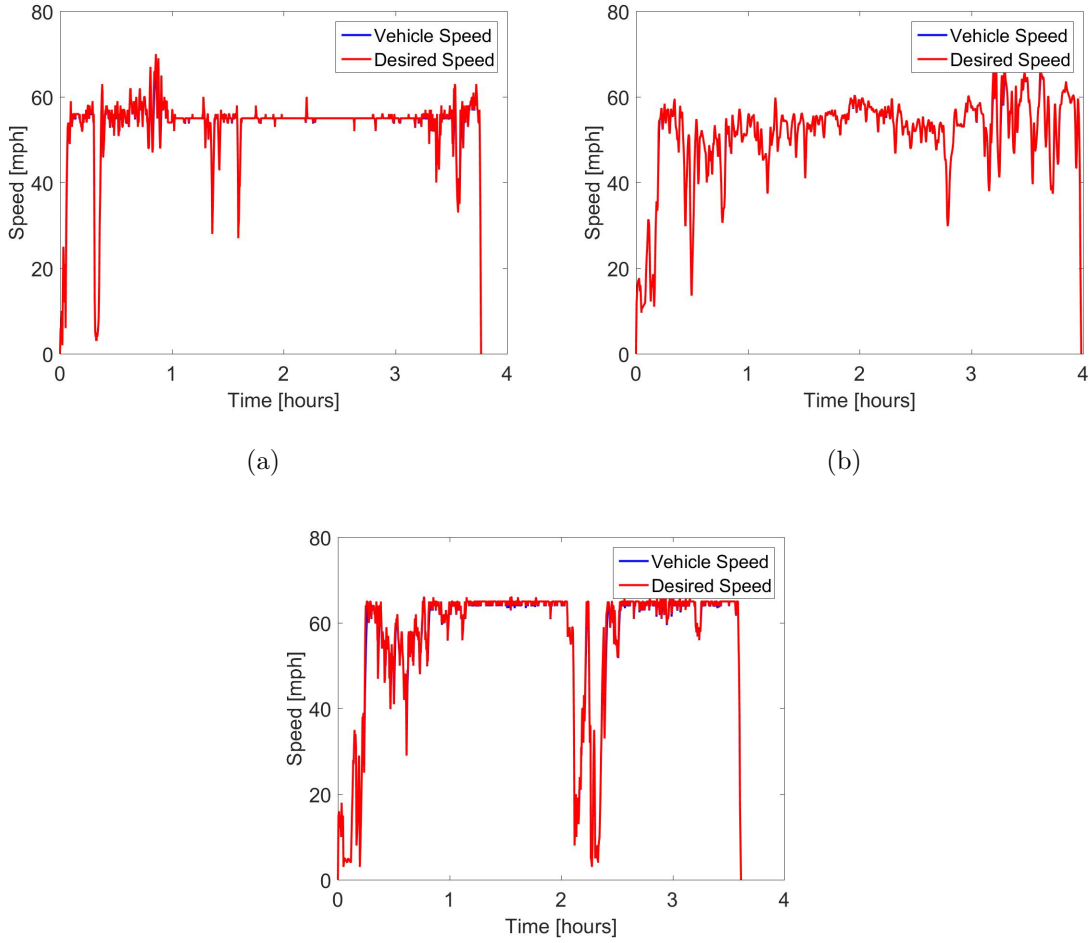

Figure 3.11. Comparison of simulated vehicle speed with desired speed (a) Drive cycle 1 (b) Drive cycle 2 (c) Drive cycle 3.

variation of SOC in all three cases, comparing Figures 3.12(a), 3.12(b) and 3.12(c) show how differently SOC is varying in each of these drive cycles and it can be inferred that there is more consistent variation of SOC in drive cycle 3, as compared to drive cycles 1 and 2. This directly means that battery is used more consistently in drive cycle 3, as compared to drive cycles 1 and 2. The reason for this is because the engine power gets saturated on the drive cycle 3 since the power requirement on this drive cycle is higher than that on drive cycles 1 and 2. On the other hand, on drive cycle 1,

SOC only varies in the initial 1.5 hours of the drive cycle and again between 3.25-3.75 hours of the drive cycle. This is exactly where the speed of the vehicle always varies, as shown in Figure 3.11(a). A similar trend can be seen on drive cycle 2, where the SOC varies relatively more during the first 1.5 hours because of a fairly high variation in vehicle speed. It then hovers around the same value until 2.75 hours and starts to vary the rest of the drive cycle due to a relatively large change in vehicle speed.

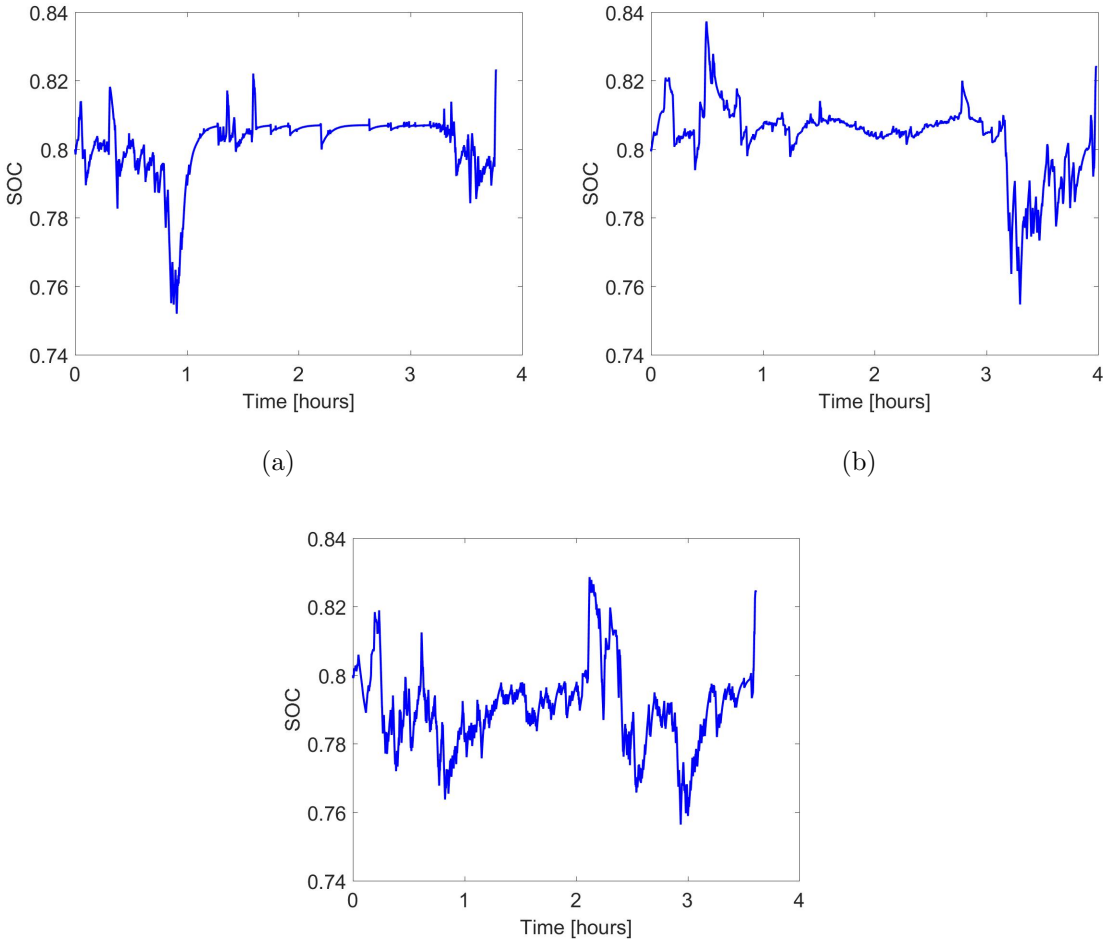

Figure 3.12. Variation of SOC (a) Drive cycle 1 (b) Drive cycle 2 (c) Drive cycle 3.

A comparison of fuel economies between a conventional heavy-duty class 8 truck and the modeled hybrid truck is shown using a bar graph in Figure 3.13. Table 3.5

Table 3.5. Fuel economy of the hybrid truck.

Drive Cycle	**Fuel Economy (mi/kg)**	**Fuel Savings (%)**
1	2.06	-0.48
2	2.05	-0.49
3	1.80	4.05

shows these fuel economy results along with % fuel savings on each drive cycle. It is observed that the hybrid truck performs better than the conventional truck in terms of fuel economy on drive cycle 3 while the fuel economy values for the hybrid on drive cycles 1 and 2 are slightly lower than those of conventional truck.

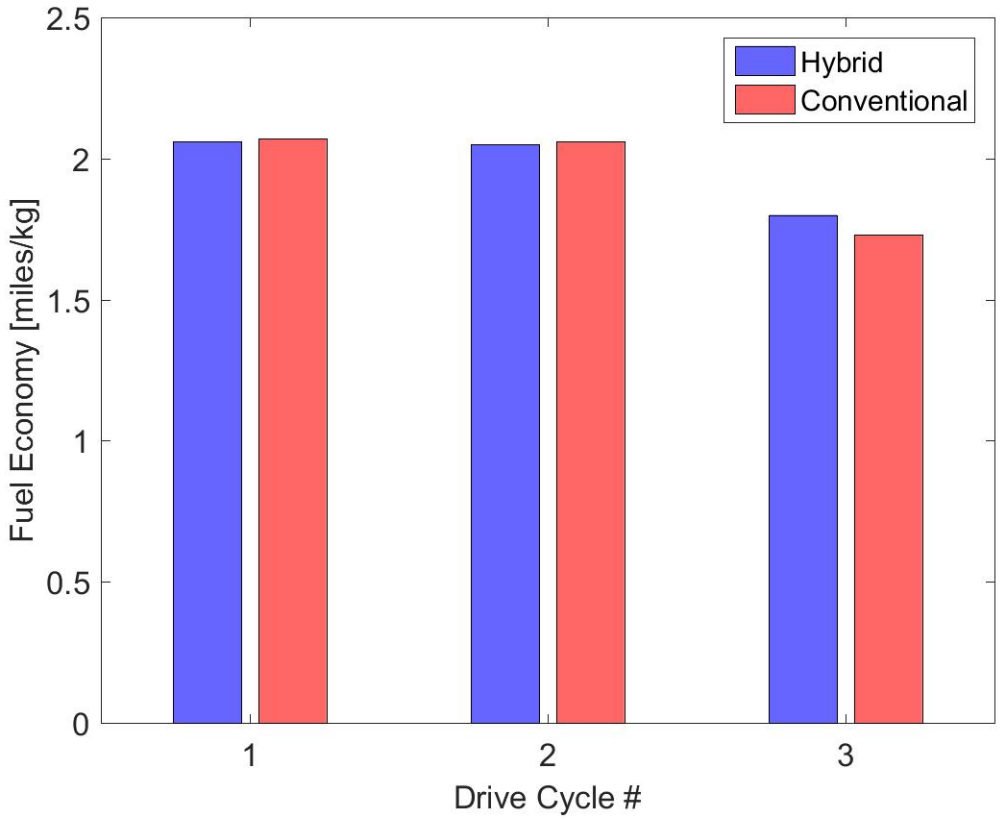

Figure 3.13. Fuel economy comparison between hybrid powertrain and conventional powertrain.

It should be remembered that hybrid powertrain has greater powertrain losses than a conventional powertrain because of the presence of additional powertrain components, such as generator and motor. For this particular combination of component sizing and control strategy, these additional losses in the hybrid powertrain force the engine to deliver higher power than what an engine in a conventional powertrain would have provided. These consistent powertrain losses for a significant period of time, without capturing any significant regenerative braking energy and not using the battery lead to a lower fuel economy than a conventional powertrain. Because of this reason, fuel economy of hybrid truck is very marginally lower than that of a conventional truck on drive cycles 1 and 2. Figure 3.14 depicts this difference of

engine powers between hybrid and conventional powertrain on drive cycle 1. It can be clearly seen that engine in hybrid powertrain has a greater power output than the engine in a conventional powertrain for a significant period of time. The reason for this difference are the additional powertrain losses. As the engine needs to deliver higher power, it burns more fuel (Figure 3.15) and this ultimately leads to fuel consumption being marginally higher than that of a conventional truck on the same route, even though there is a unique opportunity in hybrid vehicles to capture regenerative braking braking energy. A bar graph which depicts the amount of regenerative braking energy captured in a drive cycle is shown in Figure 3.17. Regenerative energy of 9.12 kWh is captured by battery on drive cycle 3, whereas in drive cycles 1 and 2, it is only 6.75 and 5.42 kWh, respectively. 35.11% more regenerative energy is captured on drive cycle 3 as compared to the regenerative energy captured on drive cycle 1 and 68.27% more regenerative energy is captured on drive cycle 3 as compared to that on drive cycle 2. This difference is a factor which leads to a better fuel economy value in drive cycle 3. Table 3.6 additionally shows the % regen energy that is captured for each of these drive cycles. It is observed that 73.4% of the regenerative energy that is available at wheel is being captured by the battery on drive cycle 1 while 67.46% and 73.97% of regenerative energy is being captured on drive cycles 2 and 3.

In Figure 3.14, there are instances of time when the engine in conventional powertrain delivers relatively higher power compared to the engine in hybrid powertrain. These are the same instances of time when the battery helps in propulsion of the vehicle in the hybrid powertrain and that is the reason SOC varies during these instances. To understand why the simulation predicts positive fuel savings on drive cycle 3 and not on drive cycles 1 and 2, powers delivered by engine in conventional powertrain and engine in hybrid powertrain drive cycle 3 are compared. This comparison is shown in Figure 3.16. It can be noticed that the engine in hybrid powertrain is operated near 200 kW most period of time on drive cycle 3. Whenever there is a requirement for more power, the battery provides power. Since the engine is saturated most of the time on this drive cycle, there is more variation in SOC on drive cycle 3 as compared

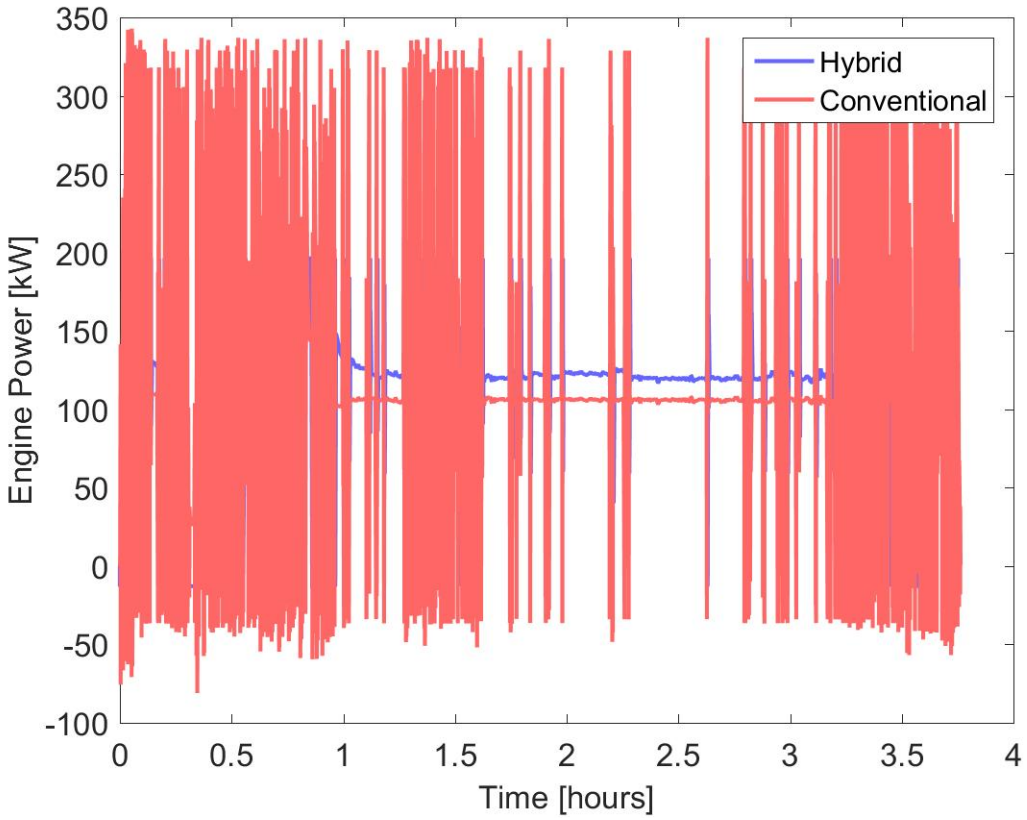

Figure 3.14. Comparison of engine powers - Drive cycle 1.

to drive cycles 1 and 2 (see Figure 3.12). Therefore, requirement of high power, assistance from battery and capturing significantly higher regenerative braking energy ultimately help in saving fuel on drive cycle 3.

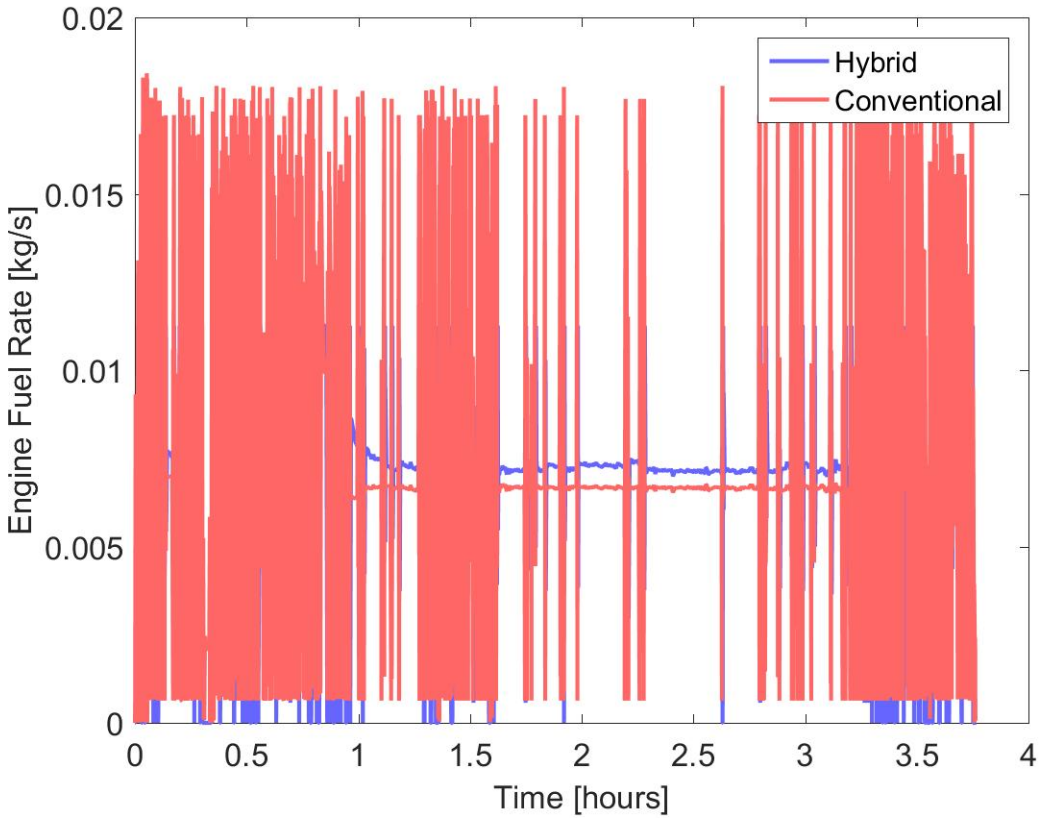

Figure 3.15. Comparison of engine fuel rates - Drive cycle 1.

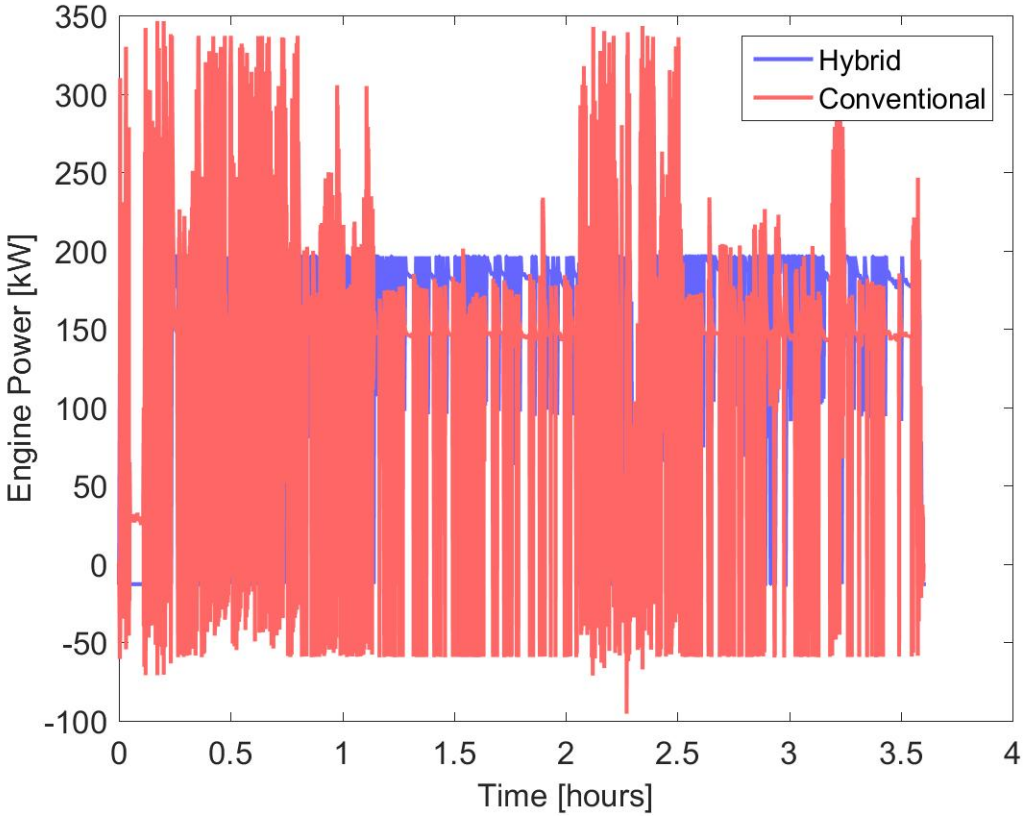

Figure 3.16. Comparison of engine power - Drive cycle 3.

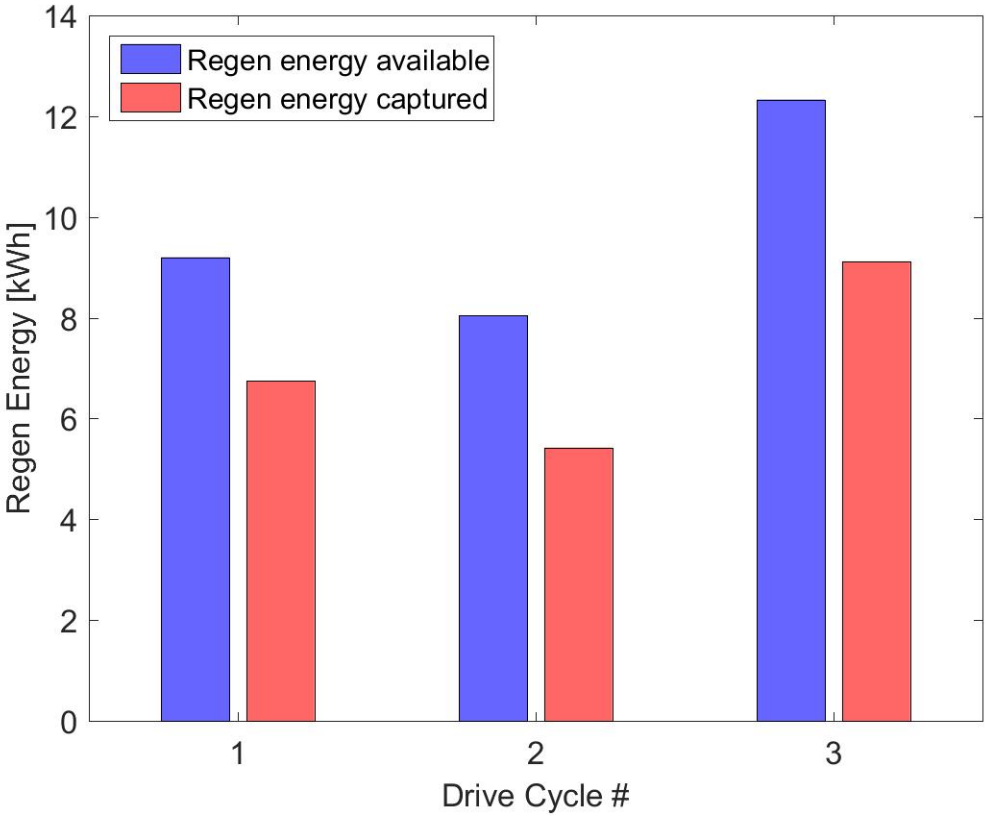

Figure 3.17. Regenerative braking energy captured.

Table 3.6. % Regen energy captured.

Drive Cycle	**Regen Available (kWh)**	**Regen Captured (kWh)**	**% Captured**
1	9.20	6.75	73.40
2	8.04	5.42	67.46
3	12.33	9.12	73.97

Since HEVs offer an opportunity to downsize the engine and use the battery when needed, examining engine efficiency gives an idea about how downsizing the engine is beneficial in terms of engine efficiency. A comparison of instantaneous engine efficiency between engine in the hybrid and the engine in conventional truck is depicted using a histogram in Figure 3.18. From Figures 3.18(a), 3.18(b) and 3.18(c), it can be concluded that hybridization allows the engine to be operated at a significantly higher efficiency point on average and the most difference in engine efficiency between hybrid and conventional trucks is noticed in drive cycle 3 where the engine in hybrid operates almost always near 40% efficiency while the engine in conventional truck operates at only around 33%. Unlike in drive cycle 3, in drive cycles 1 and 2, although the engine in hybrid is operated with a higher efficiency on average, the difference is not much as compared to drive cycle 3.

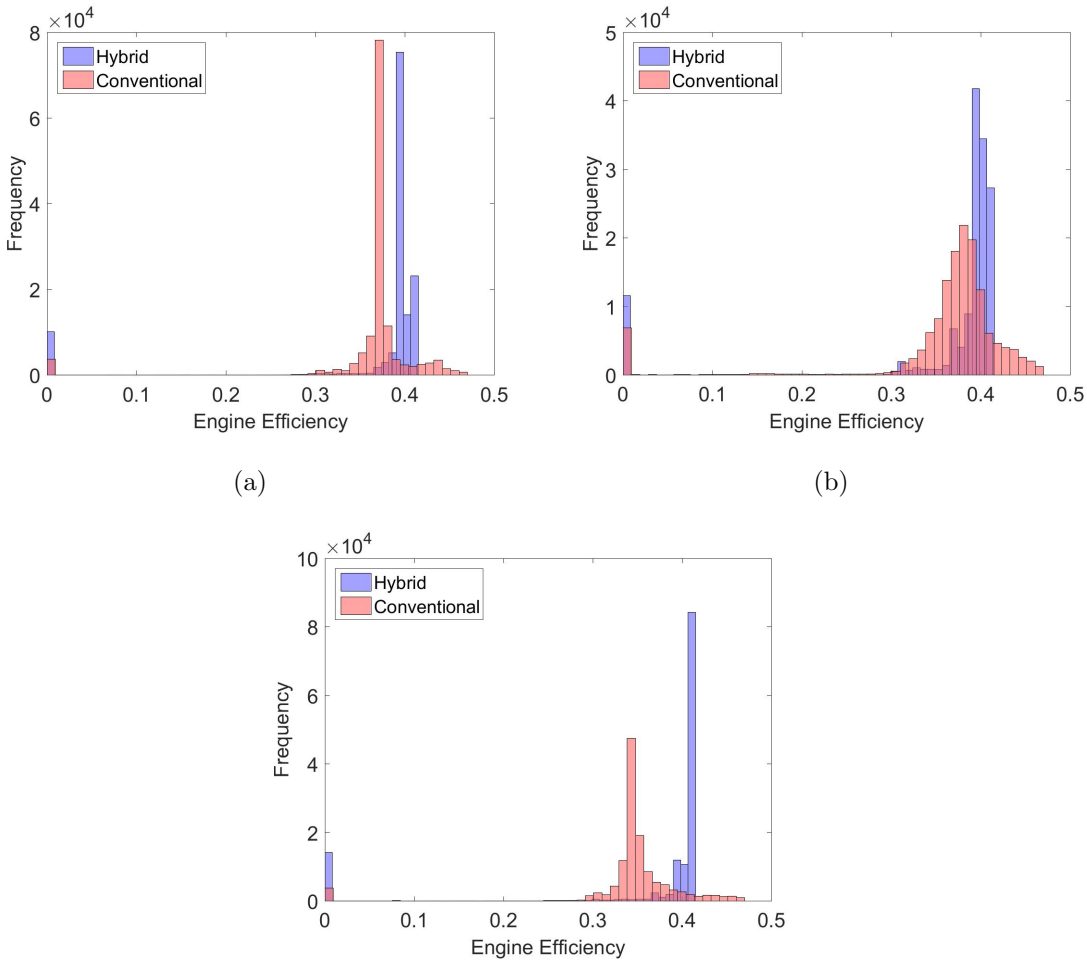

Figure 3.18. Comparison of instantaneous engine efficiency (a) Drive cycle 1 (b) Drive cycle 2 (c) Drive cycle 3.

3.5.4 Original Prototype Powertrain - Test of Gradeability

Even though the powertrain described is designed for this particular route between Florence, Kentucky and Cambridge, Ohio and is able to meet the trace requirement while maintaining SOC, it is mandatory for a truck to pass the gradeability requirement as well to enter the global market. This test requires the powertrain to be able to propel the vehicle at 20 mph while being able to resist a 7% road grade.

Interestingly, the modeled powertrain designed based on the prototype truck is not able to pass the gradeability test even though it works well on previously described drive cycles. A comparison between required speed to pass gradeability test and actual vehicle speed is shown below in Figure 3.19. It can be seen that the simulated vehicle is only able to reach a speed of around 18 mph with a road grade of 7%. The initial part of the vehicle speed can be thought of as an acceleration delay since the vehicle cannot reach the desired speed instantaneously, when there is such a large difference between the desired speed in the following instant of time.

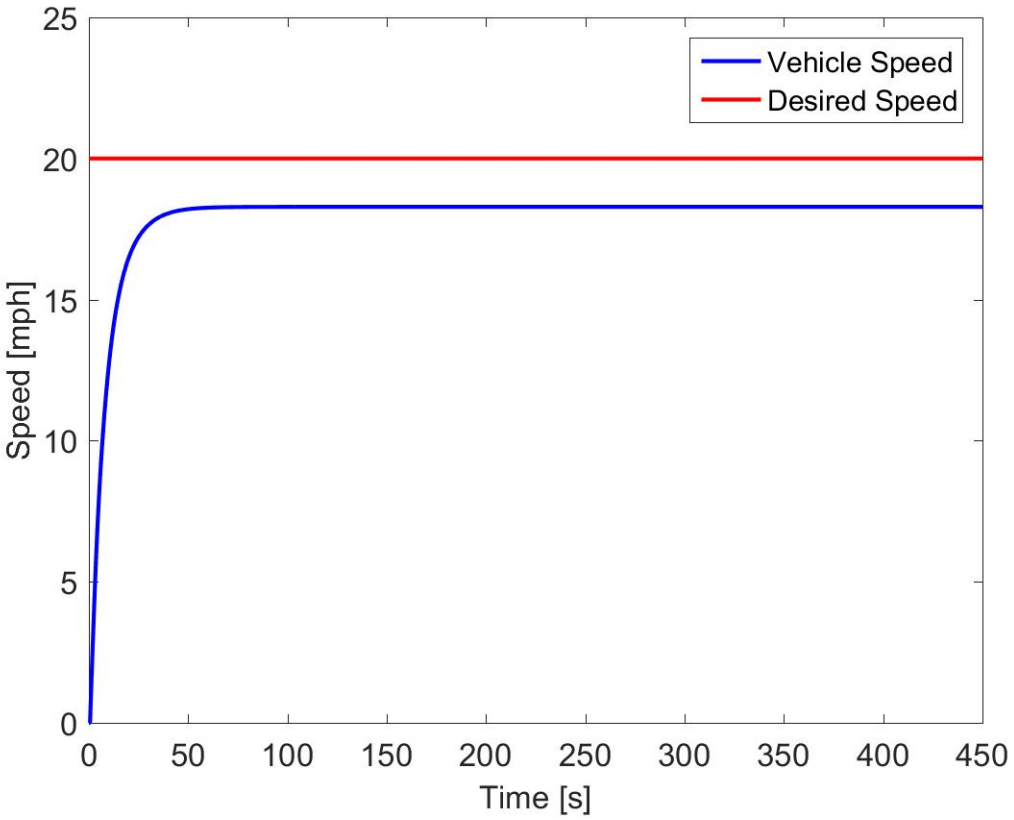

Figure 3.19. Vehicle speed trace for gradeability test.

The reason for being unable to meet the gradeability requirement is because of power limitation of the motor, which is only sized to be 150 kW. Simply inspecting the tractive power requirement conveys that motor peak power is not enough to deliver

required tractive power. The tractive power required to pass the gradeability test is around 155.5 kW while the motor can only deliver a peak power of 150 kW. It should also be noted that this tractive power required is just calculated considering aerodynamic, rolling and grade losses. Additionally, there are powertrain losses that are not taken into consideration while computing tractive power requirement. Therefore, it is crucial that the powertrain components are sized appropriately to meet both the trace requirement and gradeability requirement.

3.5.5 Powertrain with Increased Motor Peak Power

Since the reason for not being able to meet the gradeability criterion was the motor peak power, the same powertrain but with increased motor peak power was tested for gradeability. The motor peak power of 150 kW in the original powertrain was changed to 175 kW while keeping the other powertrain parameters same. It can be seen from Figure 3.20 that increasing the motor peak power to 175 kW allows the vehicle to pass the gradeability test. Although the vehicle is now able to meet the gradeability requirement, the fuel economy (shown in Table 3.7) is observed to be the same as the original powertrain, which is anticipated because only the motor size has been changed which doesn't affect the operation of the engine and battery significantly.

Table 3.7. Fuel economy of the powertrain with increased motor peak power.

Drive Cycle	**Fuel Economy (mi/kg)**	**Fuel Savings (%)**
1	2.06	-0.48
2	2.05	-0.49
3	1.80	4.05

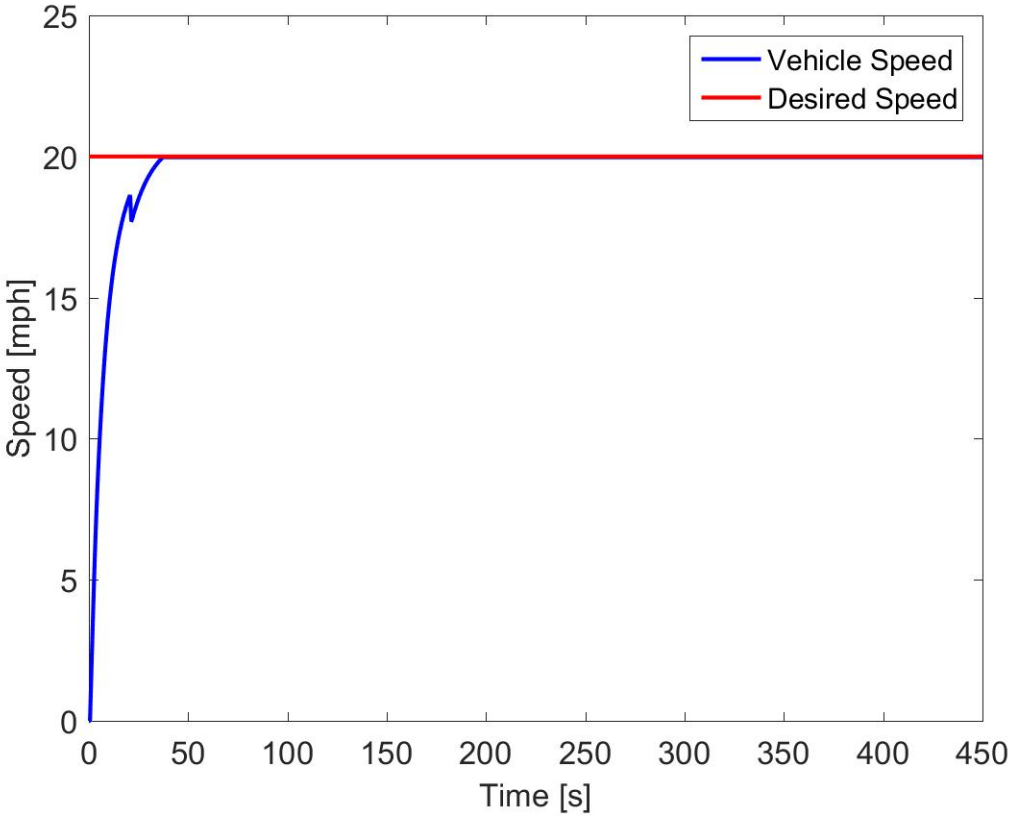

Figure 3.20. Gradeability test - Motor peak power increased to 175 kW.

3.5.6 Modified Powertrain

In an effort to meet the gradeability requirement and also achieve better fuel economy, the component sizes in the powertrain (engine generator, motor and battery) have been modified and the modified parameters of the powertrain are listed in Table 3.8. More precisely, the engine and generator have been downsized to 200 kW while the motor peak power has been increased to 175 kW to meet the gradeability requirement. Also, the battery size has been doubled from 25.67 kWh to 51.34 kWh. As a reminder, the engine in the original powertrain was being operated between 1700-1900 RPM and the peak engine power in that range was 209 kW. Therefore, to the attain same level of engine power, the engine in the modified powertrain is operated

between 2400-2600 RPM instead of 1700-1900 RPM. As long as the vehicle is able to meet the performance criteria, downsizing the engine is also beneficial during low load requirements where the engine efficiency is generally low.

In order to allow the battery to charge/discharge quickly and maintain the SOC strictly, the battery power demand is also modified. The modified map is shown in Figure 3.21. Changing the battery power demand curve results in the battery having to supply/demand more power and this means that SOC of battery is regulated quicker. The slope of the curve essentially dictates how aggressively the SOC is regulated. As the slope is increased, battery supplies/demands more power than it would without such a high slope which results in reaching the target SOC faster. Also, increasing the number of cells in the battery pack not only increases the energy capacity of the battery pack but also the power supplied/demanded, since they are directly related to each other.

Table 3.8. Component sizing - Modified powertrain.

	Engine Peak Power (kW)	**Generator Peak Power (kW)**	**Motor Peak Power (kW)**	**Battery Energy Capacity (kWh)**
Original powertrain	261	261	150	25.67
Modified powertrain	200	200	175	51.34

As the first step in simulation, a test of gradeability is performed on the modified powertrain. Figure 3.22 shows the speed trace and it can be observed that the vehicle is able to reach a speed of 20 mph and then maintain the speed throughout while being able to overcome a road grade of 7%.

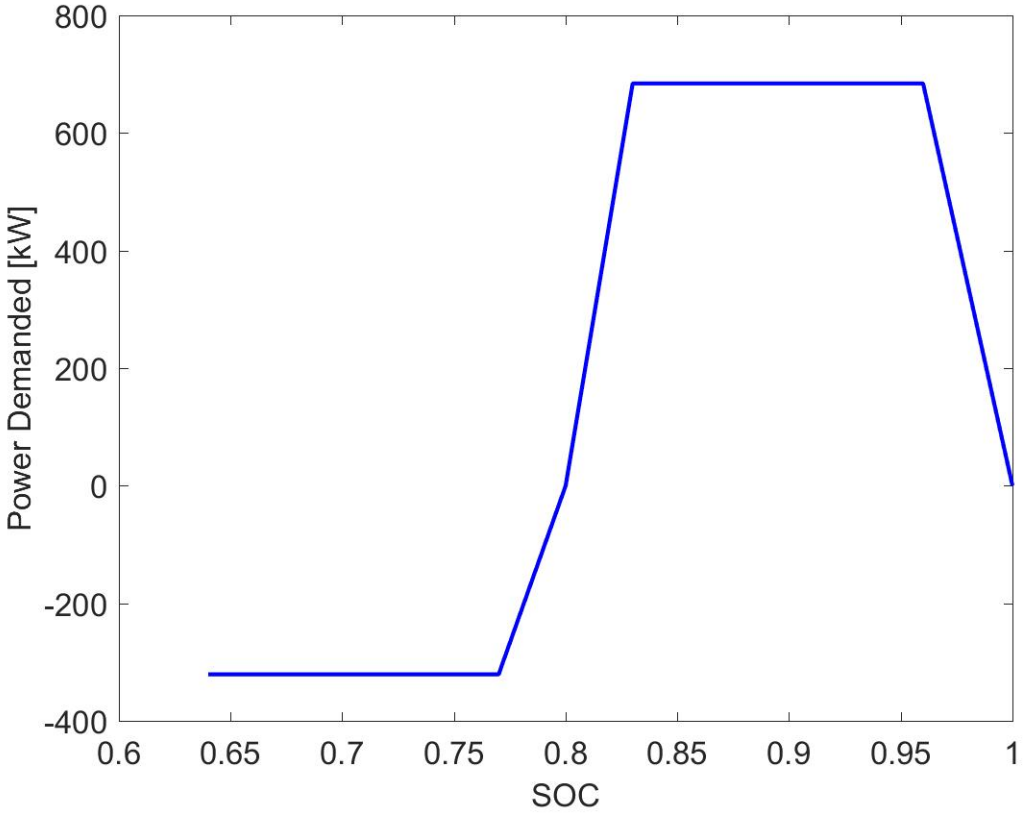

Figure 3.21. Modified battery power demand curve based on current SOC.

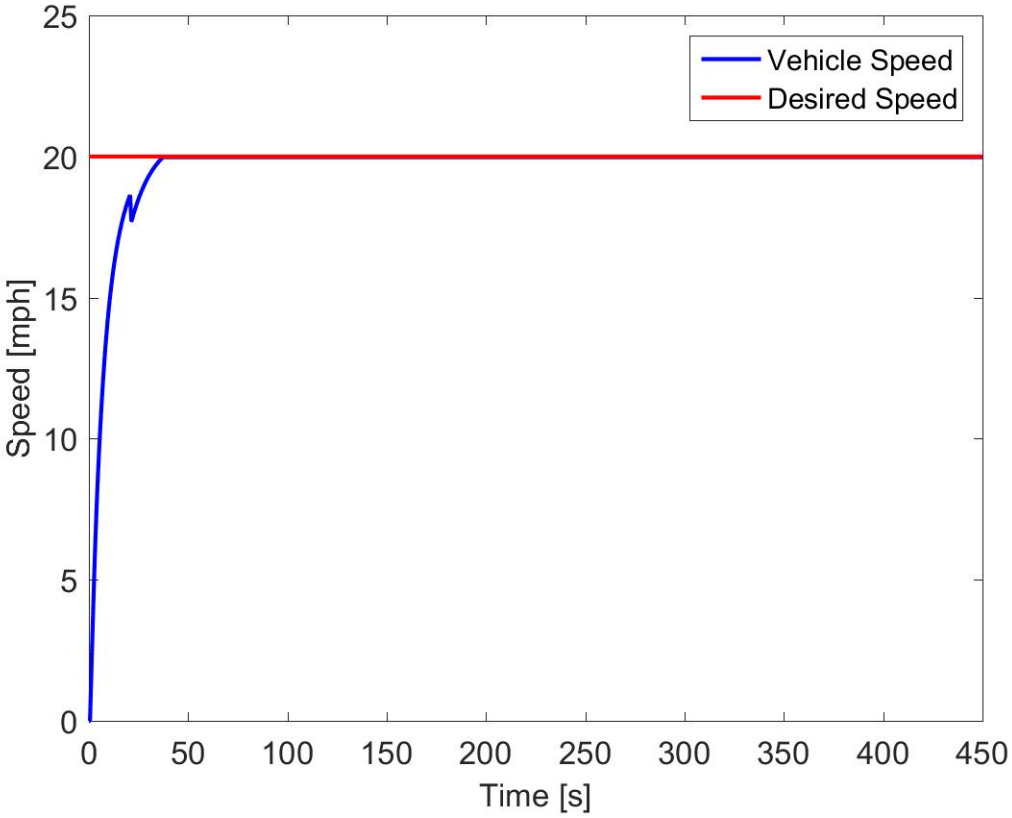

Figure 3.22. Speed trace - Gradeability.

A comparison of fuel economies considering all three powertrains namely, modified, original and conventional powertrains, is shown using a bar graph depicted in Figure 3.23. Numerical values of the same, along with fuel savings, are listed in Table 3.9. It's seen that the modified powertrain has better fuel economy as compared to baseline conventional class 8 truck on all three drive cycles considered, unlike the original powertrain which has better fuel economy only on drive cycle 3. The % fuel savings for drive cycle 3 are seen to be the highest while savings are the least on drive cycle 2, following a similar trend as before.

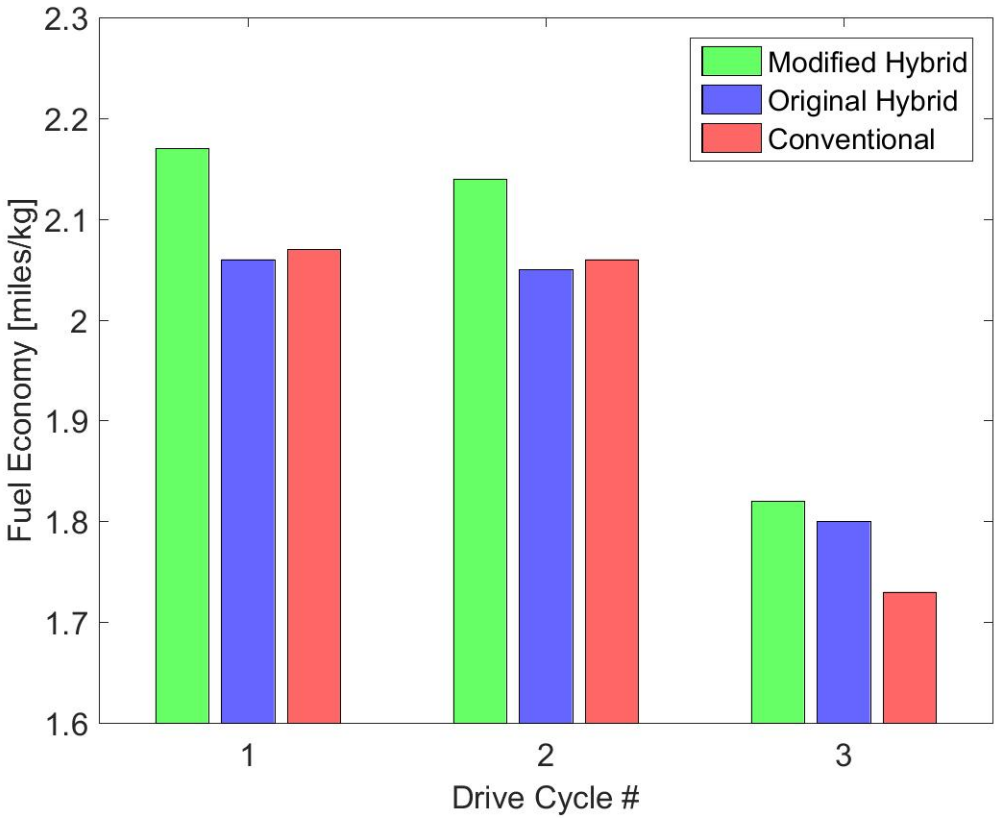

Figure 3.23. Fuel economy comparison - Modified powertrain sizing.

Table 3.9. Fuel economy of the modified truck.

Drive Cycle	**Fuel Economy Original Hybrid (mi/kg), Fuel Savings (%)**	**Fuel Economy Modified Hybrid (mi/kg), Fuel Savings (%)**
1	2.06 (-0.48)	2.17 (4.83)
2	2.05 (-0.49)	2.14 (3.88)
3	1.80 (4.05)	1.82 (5.20)

Figure 3.24 shows how the SOC is being regulated on all three drive cycles. It can be easily noticed that the SOC is maintained much more strictly through out the course of each drive cycle when compared to Figure 3.12. Again, SOC is found to vary more during those periods of time where there is a variation of vehicle speed, similar to how it was in original hybrid. But this variation is much sharper due to the change in power demand curve of the battery, as expected. Also, it can be noticed that the engine operating points are concentrated more towards the maximum power curve on drive cycle 3 when compared to drive cycles 1 and 2.

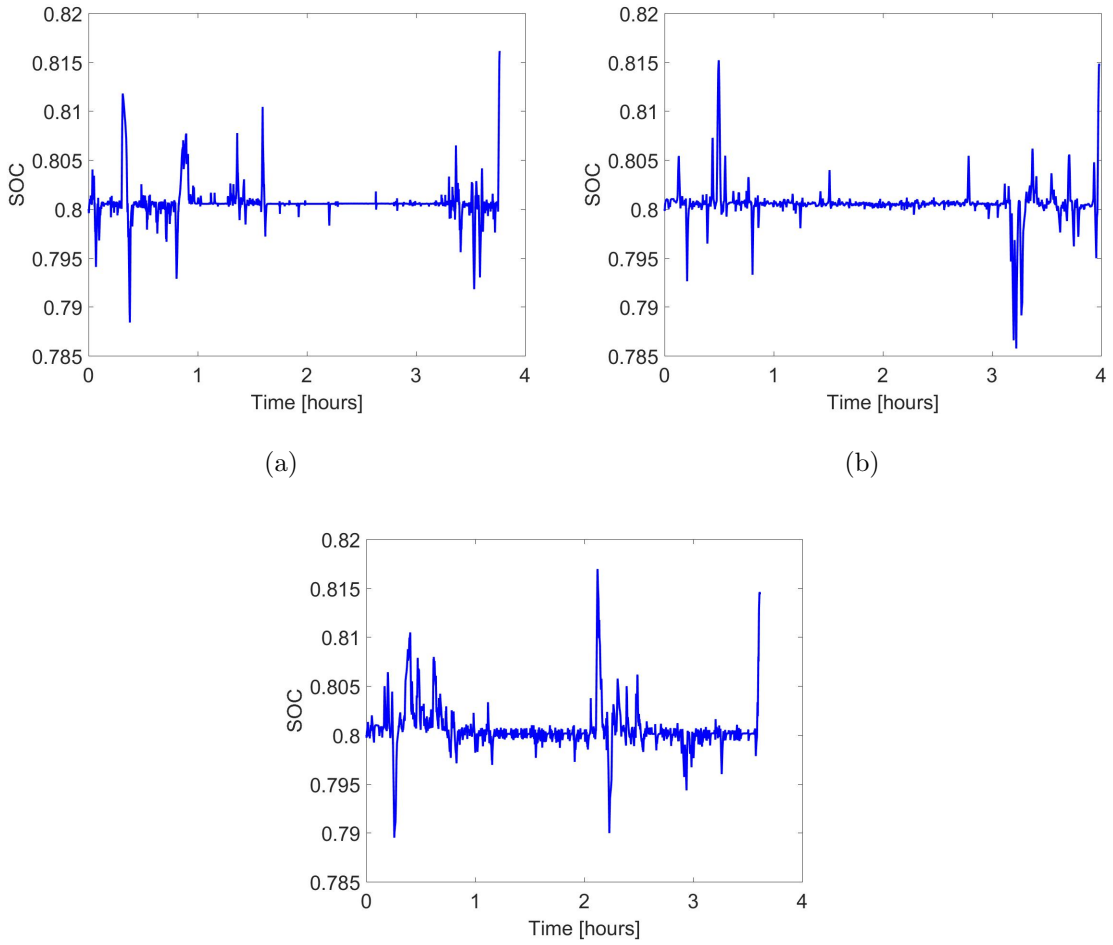

(a)

(b)

(c)

Figure 3.24. Variation of SOC - Modified powertrain (a) Drive cycle 1 (b) Drive cycle 2 (c) Drive cycle 3.

Figure 3.25 depicts the range of engine operation in the modified hybrid powertrain. Visibly, the engine operates between 2400-2600 RPM close to the maximum power curve but never exceeding the power limit of the engine, as intended.

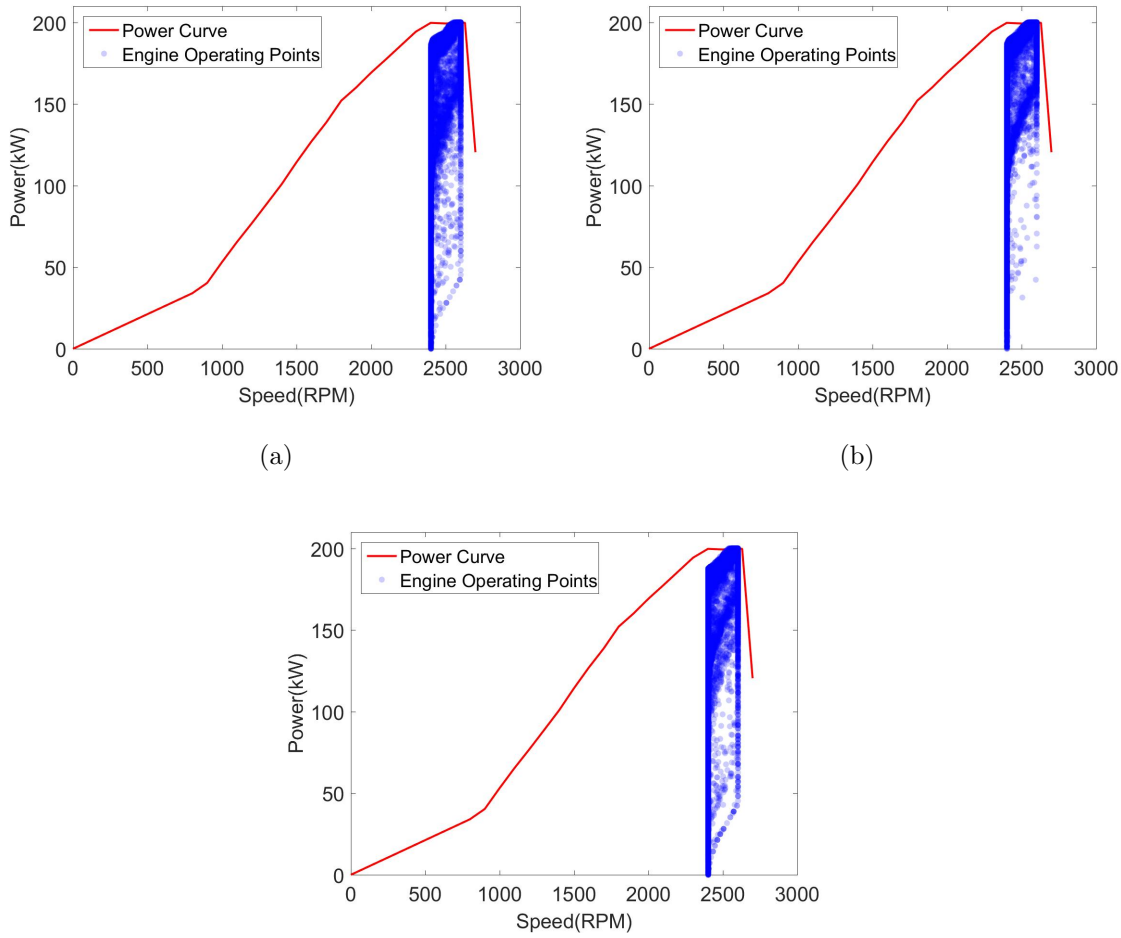

Figure 3.25. Engine operating range - Modified powertrain (a) Drive cycle 1 (b) Drive cycle 2 (c) Drive cycle 3.

Figure 3.26 shows a histogram comparing efficiency of engine in modified hybrid powertrain and engine in class 8 conventional powertrain. It can be seen that engine operates at a higher efficiency point when compared to the baseline conventional powertrain and this difference is seem predominantly on drive cycle 3, following the same trend as the original hybrid powertrain did. It is a known fact that higher engine efficiency is reached at power values close to rated power in the engine map. As the power requirement for drive cycle 3 is significantly higher as compared to drive cycles

1 and 2, engine operates at an efficiency close to 0.4 most of the time on drive cycle 3 and not as much on drive cycles 1 and 2 . Although the average engine efficiency of modified hybrid powertrain is slightly lower than that of the original powertrain, the modified hybrid has better fuel economy. This is because the engine in the modified hybrid is being operated at a lower power as compared compared to the one in original hybrid powertrain (shown in Figure 3.27). It can be understood that, although the engine in the modified powertrain delivers slightly higher power than the engine in a conventional truck, this difference is significantly less than the difference between the engine in original powertrain and engine in conventional powertrain. This reduction of power delivered results in a decrease in fuel burn rate as well as a small reduction in engine efficiency. A comparison of fuel burn rates of engines in original hybrid, modified hybrid and conventional powertrains is depicted in Figure 3.28. A similar decrease in fuel burn rate (shown in Figure 3.29) is seen on drive cycle 3 as well, leading to more fuel savings as compared to original hybrid powertrain.

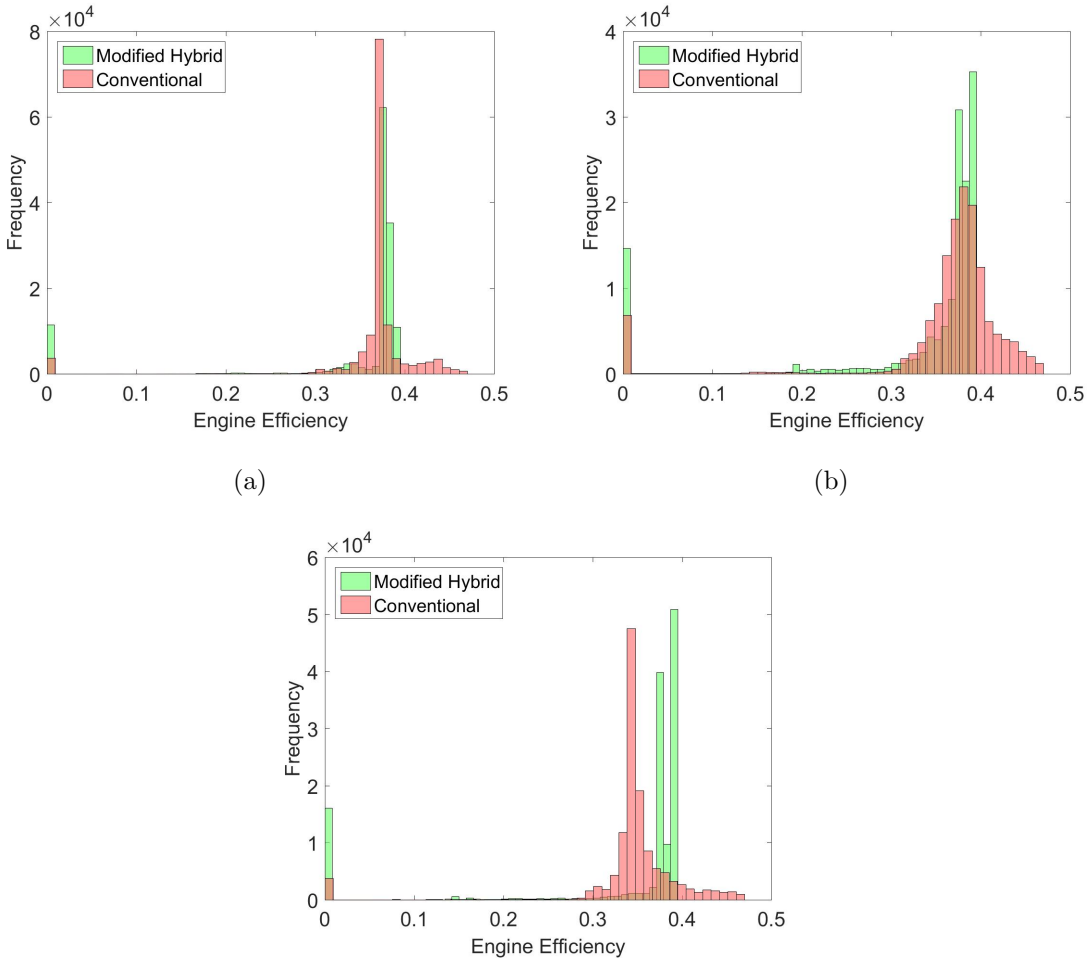

Figure 3.26. Comparison of instantaneous engine efficiency - Modified powertrain (a) Drive cycle 1 (b) Drive cycle 2 (c) Drive cycle 3.

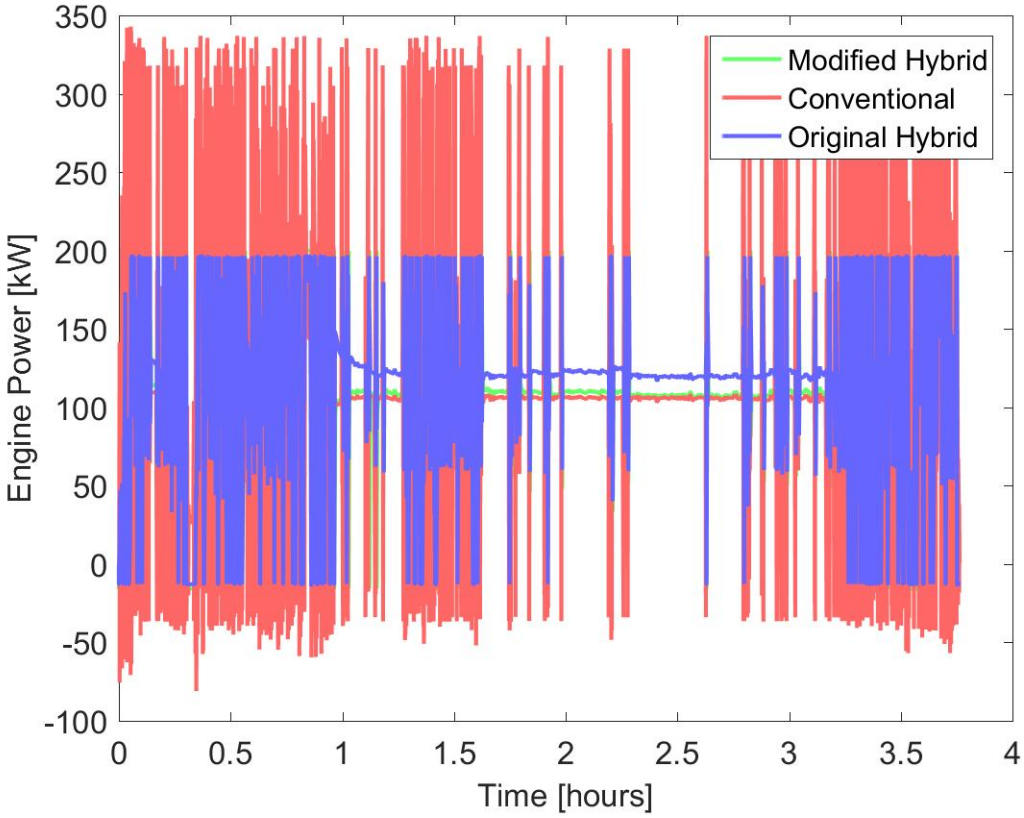

Figure 3.27. Engine power comparison - Modified hybrid - Drive cycle 1.

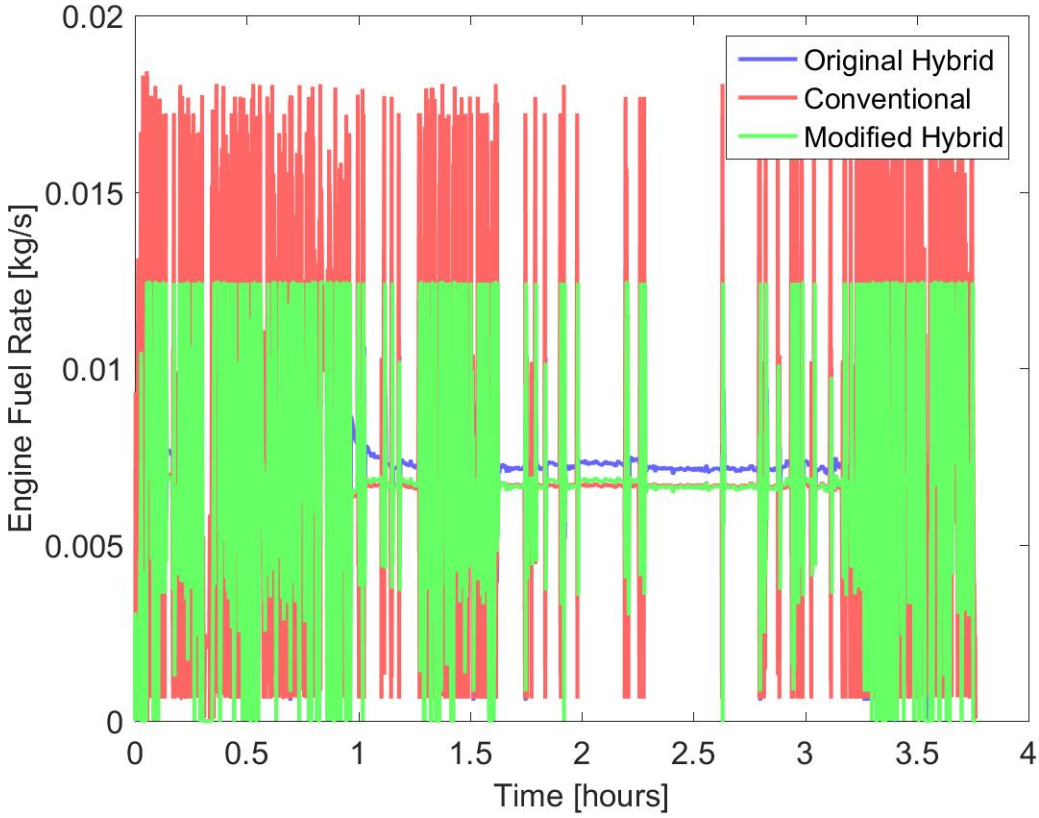

Figure 3.28. Engine fuel rate comparison - Modified hybrid - Drive cycle 1.

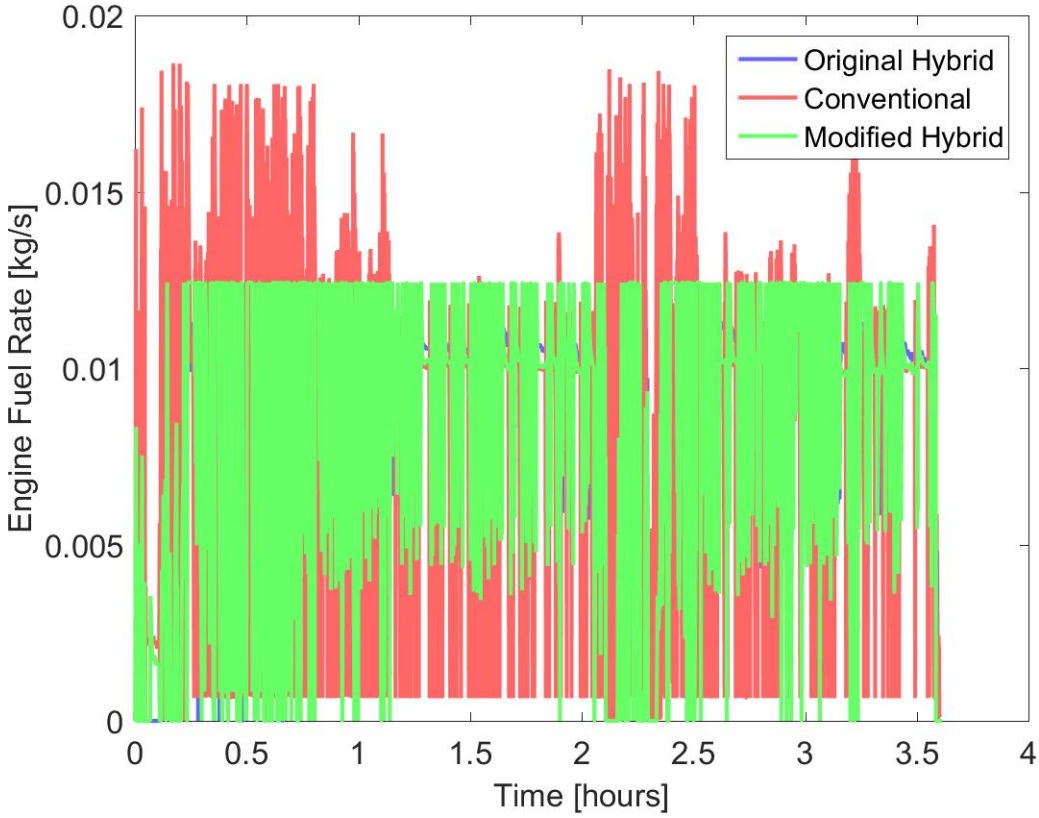

Figure 3.29. Engine fuel rate comparison - Modified hybrid - Drive cycle 3.

3.6 Possible Reasons for Not Matching Experimental Fuel Economy

A comparison of how accurate the fuel consumption prediction for the original powertrain by Autonomie is, as compared to the experimental results, is shown in Table 3.10. As a reminder, drive cycle 3 is the only drive cycle of all the experimental tests where a conventional package delivery tractor has been used. Since it is a conventional powertrain, the fuel economy value is compared with the simulation result of a conventional powertrain.

Table 3.10. Comparison of simulated fuel economy with experimental results.

Drive Cycle	**Tractor/ Driver**	**Experimental Fuel Economy (mi/kg)**	**Simulated Fuel Economy (mi/kg)**
1	Prototype/Start-up	2.23	2.06 (Hybrid)
2	Prototype/Package Delivery	2.11	2.05 (Hybrid)
3	Package Delivery/Package Delivery	1.72	1.73 (Conventional)

Fuel economy values of Autonomie prediction of conventional truck and conventional package delivery tractor match quite closely, while on drive cycles 1 and 2 where the prototype tractor was used, it doesn't match as well. The most likely reason for this discrepancy is the unavailability of the energy management control strategy that was being used in the prototype truck and it is likely that the control strategy that is being used in Autonomie is different from what is used in the prototype. It is known that fuel economy is sensitive to the vehicle energy management control strat-

egy being used. [8], [11], [12] explore the effects of various control strategies on fuel economy of the vehicle. Another likely reason for this dissimilarity in fuel economy is because of the possibility that the prototype tractor could have a drag coefficient (C_D) less than 0.6 (value of C_D used in Autonomie simulation). The aerodynamic drag force that acts on a vehicle, $\frac{1}{2}C_D\rho Av^2$ is proportional to the square of vehicle velocity and consequently, the power needed to overcome this force is proportional to the cube of vehicle velocity. Any small difference in truck aerodynamics can lead to a significant difference in fuel economy, as heavy-duty trucks travel at high-way speeds with a high frontal area. The prototype tractor and the package delivery tractor are aerodynamically very different. On drive cycle 1, by assuming a C_D value of 0.55 while keeping every other parameter exactly the same, the simulation predicts a fuel economy of 2.165 miles/kg. A similar trend can be observed on drive cycle 2 as well, where by assuming a C_D value of 0.55, the simulation predicts a fuel economy of 2.14 (shown in Table 3.11).

Table 3.11. Fuel economy sensitivity to drag coefficient.

Drive Cycle	**Tractor/Driver**	**Fuel Economy (mi/kg) with C_D = 0.6**	**Fuel Economy (mi/kg) with C_D = 0.55**
1	Prototype/Start-up	2.06 mi/kg	2.17 mi/kg
2	Prototype/Package delivery	2.05 mi/kg	2.14 mi/kg

A difference of 5.34% and 4.39% is seen on drive cycle 1 and drive cycle 2, solely due to the change in C_D. The high possibility of aerodynamic drag coefficient being different for the prototype tractor than the assumed value of 0.6, along with the energy management control strategy being different could lead to this difference in fuel economy values. Also, as mentioned earlier, the initial and final SOCs of the

battery during the experimental testing of the prototype truck are uncertain. This could lead to a considerable change in the fuel economy value.

3.7 Effect of Drive Cycle on Fuel Economy

It has been determined that there is little/no benefit in terms of fuel economy due to hybridization on any of the three drive cycles considered. To check if a similar trend would be seen on other drive cycles also and to understand the effect of drive cycle on the fuel economy on a hybrid powertrain, the original powertrain model has been simulated on four standard drive cycles which represent city-style driving (high number of acceleration/deceleration events). The drive cycles considered for this analysis are Urban Dynamometer Driving Schedule (UDDS) drive cycle, Orange County drive cycle, Manhattan drive cycle, and New York Composite drive cycle. The speed profiles for these drive cycles are depicted in Figures 3.30 - 3.33. It can be seen clearly that the number of stops, acceleration and deceleration events for these drive cycles are comparatively much higher than those in drive cycles that were considered earlier.

Figure 3.34 shows a bar graph comparing the fuel economy of hybrid powertrain with a conventional powertrain on each of these four drive cycles. The numerical values of fuel economy for both hybrid and conventional powertrains are shown in Table 3.12. It's observed that there are fuel savings of 16.9%, 19.5%, 17.1%, 12.8% on UDDS, Orange County, Manhattan, NY Composite drive cycles, respectively, with exactly the same powertrain and power management control strategy as the original powertrain. Fuel savings observed on these drive cycles are notably higher as compared to the fuel savings of the same hybrid powertrain on highway style drive cycles.

It is also seen that the regenerative braking energy captured, considering the total duration of drive cycle time (shown in Figure 3.35 and Table 3.13) on all of these drive cycles is substantially greater than that captured on highway style drive cycles.

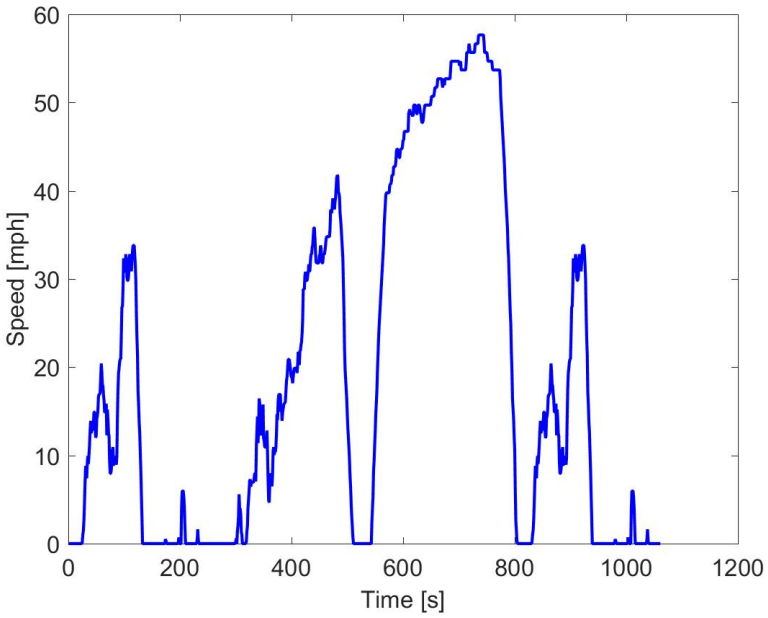

Figure 3.30. UDDS Drive Cycle.

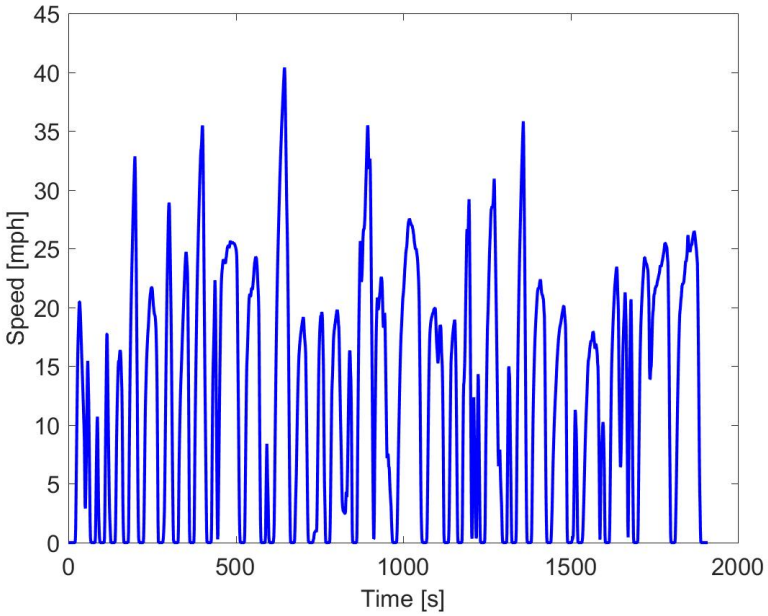

Figure 3.31. Orange County Drive Cycle.

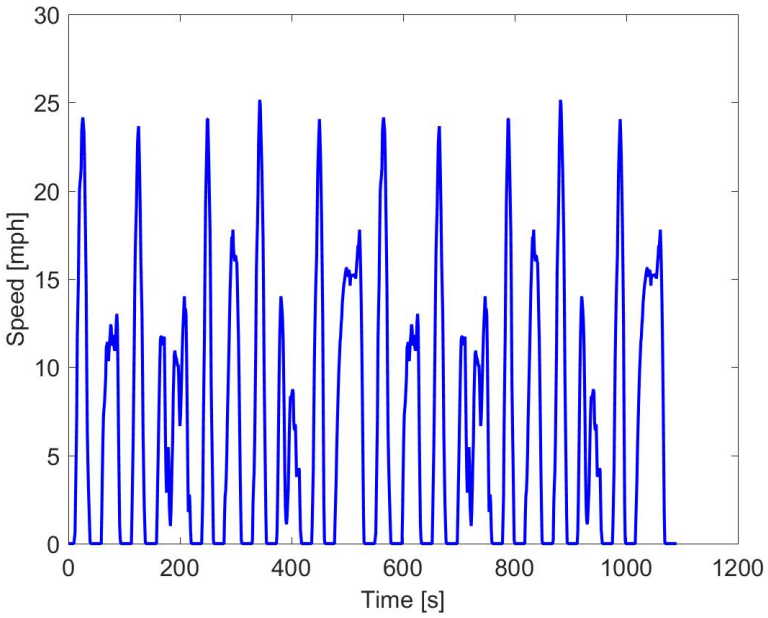

Figure 3.32. Manhattan Drive Cycle.

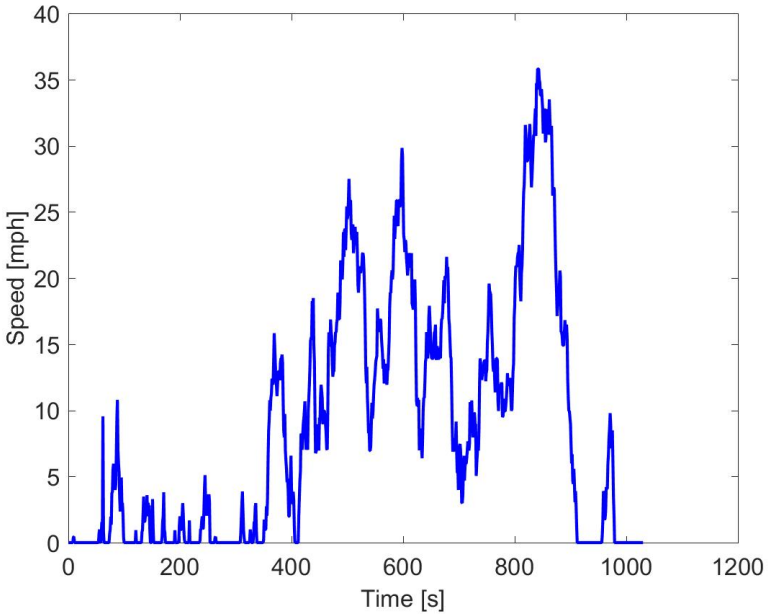

Figure 3.33. NY Composite Drive Cycle.

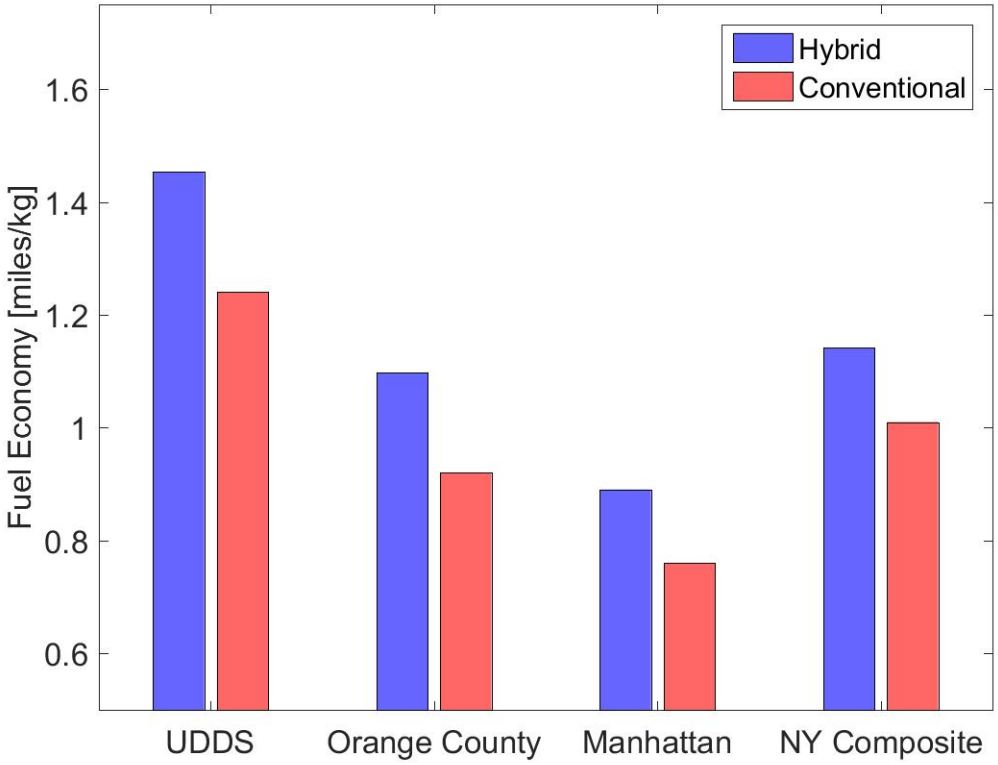

Figure 3.34. Fuel economy comparison.

Table 3.12. Effect of drive cycle on fuel economy.

Drive Cycle	**Fuel Economy - Hybrid [mi/kg]**	**Fuel Economy - Conventional [mi/kg]**
UDDS	1.45	1.24
Orange County	1.10	0.92
Manhattan	0.89	0.76
NY Composite	1.14	1.01

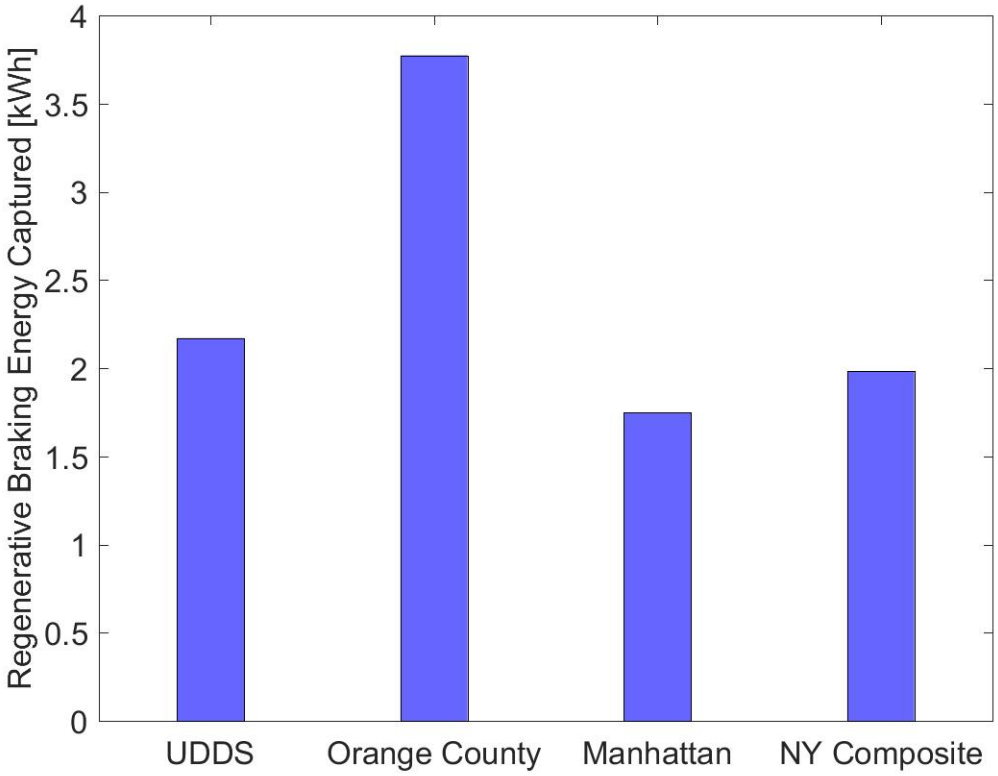

Figure 3.35. Regenerative braking energy captured.

Table 3.13. Regen energy captured on city-style drive cycles.

Drive Cycle	**Regenerative Braking Energy Captured [kWh]**
UDDS	2.17
Orange County	3.77
Manhattan	1.75
NY Composite	1.98

The regenerative energy captured on these drive cycles is low in terms of magnitude

Table 3.14. Comparison of normalized regen energy captured.

Drive Cycle	**Normalized Regen Energy Captured [Wh/s]**
UDDS	2.045
Orange County	2.043
Manhattan	1.607
NY Composite	1.924
Drive cycle 1	0.497
Drive cycle 2	0.377
Drive cycle 3	0.701

but it should be noted that these drive cycles have a total duration of only 20-30 minutes, whereas the highway-style drive cycles considered had a total duration of around 4 hours.

To show this, the regen energy captured on all drive cycles under consideration is normalized with time and is shown in Table 3.14. Because of high number of stops, there are significantly more opportunities for capturing braking energy which has a direct effect on fuel savings on these drive cycles.

4. CONCLUSIONS AND FUTURE WORK

4.1 Conclusions

This study was performed to investigate the potential fuel savings due to powertrain electrification in class 8 heavy-duty trucks. A newly developed series electric hybrid powertrain by a start-up was the powertrain of interest. Several tests were performed on a route between Florence, Kentucky and Cambridge, Ohio to determine the experimental fuel economy of the prototype truck. Additionally, reasons for variation in fuel economy results between each test performed during this phase are presented.

Although experimental testing provided information such as fuel economy and route, a vehicle simulation model was created and simulated in Autonomie in order to evaluate % fuel savings. This was done because there was no real-world test performed using a similar velocity profile and GVW. Of all the drive cycle information obtained from real-world testing, three drive cycles each representing a driving speed and style were selected to perform the simulation. The results from simulation also provided further insight into the operation of the electric hybrid powertrain. It was determined that the modeled powertrain performs better than a conventional truck in terms of fuel economy only on drive cycle 3, which is a 65 mph drive cycle. On the other two drive cycles, the fuel economy of the hybrid powertrain was found to be very marginally lower than a conventional powertrain. On all three drive cycles considered, powertrain hybridization allowed the engine to be operated at a higher efficiency value when compared to conventional truck. This did not necessarily translate to fuel savings because of consistent losses within the additional powertrain components such as generator and motor, which are absent in a conventional powertrain. Furthermore, it was discovered that the hybrid powertrain modeled in Autonomie was not able to pass

the gradeability criterion. After troubleshooting, it was established that motor peak power is not sufficiently high to pass this requirement. A powertrain with increased motor peak power, while keeping the other component sizes the same was tested for gradeability and it was observed that increased motor peak power allowed the vehicle to meet the gradeability requirement. It was also seen that this powertrain performed very similarly to the original powertrain in terms of fuel economy. Therefore, a modified powertrain with reduced engine-generator size, increased motor and battery size was modeled and investigated on these same routes. This powertrain performed better than a conventional powertrain on all three routes because of the combined effect of engine downsizing and increase in battery size. Also, this powertrain was able to meet the gradeability criterion. Towards the end of the thesis, the predicted fuel economy by Autonomie is compared to that obtained from experimental testing and likely reasons for the simulation not being to able to match the experimental fuel economy results are provided. The effect of drive cycle on fuel economy is also studied by considering city-style speed profiles instead of highway-style driving. It was determined that hybridizing a powertrain is beneficial on drive cycles with high number of stops because of an increased opportunity for capturing regenerative braking energy, which would otherwise be lost in a conventional powertrain.

4.2 Scope for Future Work

- Access to the energy management control strategy that is being used in the experimental truck would help in performing a similar analysis in a much more accurate way. Since the application of interest is freight transportation, other existing control strategies can be evaluated for this architecture which could aid in designed the best control strategy with respect to fuel economy.

- Saving fuel due to powertrain electrification does not certainly mean that electrification is beneficial economically. This is because a hybrid powertrain has an higher initial cost, due to added powertrain components such as generator,

motor and battery. In order to identify global market opportunities for a newly designed powertrain, a complete economic analysis needs to be performed for that particular powertrain while taking into account operation uncertainties.

- The change in powertrain component sizes to create the modified hybrid powertrain was heuristic. There is scope to perform a more systematic component sizing design in order to evaluate the optimal powertrain component sizing.

REFERENCES

[1] Climatic Research Unit.

[2] NASA Global Climate Change.

[3] United States Energy Information Administration. Annual Energy Outlook 2017.

[4] C. Mi and M. Masrur. *Hybrid electric vehicles: principles and applications with practical perspectives*. John Wiley & Sons, 2017.

[5] M. Yoong, Y. Gan, G. Gan, C. Leong, Z. Phuan, B. Cheah, and K. Chew. Studies of regenerative braking in electric vehicle. In *Sustainable Utilization and Development in Engineering and Technology, 2010 IEEE Conference*. IEEE, 2010.

[6] H. Zhao, A. Burke, and M. Miller. Analysis of class 8 truck technologies for their fuel savings and economics. *Transportation Research Part D: Transport and Environment*, 23:55–63, 2013.

[7] P. Tulpule, V. Marano, and G. Rizzoni. Effects of different phev control strategies on vehicle performance. In *American Control Conference, 2009. ACC'09.*, pages 3950–3955. IEEE, 2009.

[8] L. Serrao, S. Onori, and G. Rizzoni. A comparative analysis of energy management strategies for hybrid electric vehicles. *Journal of Dynamic Systems, Measurement, and Control*, 133(3):031012, 2011.

[9] S. Di Cairano, D. Bernardini, A. Bemporad, and I. Kolmanovsky. Stochastic mpc with learning for driver-predictive vehicle control and its application to hev energy management. *IEEE Trans. Contr. Sys. Techn.*, 22(3):1018–1031, 2014.

[10] O. Tremblay, L. Dessaint, and A. Dekkiche. A generic battery model for the dynamic simulation of hybrid electric vehicles. In *Vehicle Power and Propulsion Conference, 2007. VPPC 2007. IEEE*, pages 284–289. Ieee, 2007.

[11] W. Shabbir, C. Arana, and S. Evangelou. Series hybrid electric vehicle supervisory control based on off-line efficiency optimization. In *Electric Vehicle Conference (IEVC), 2012 IEEE International*, pages 1–5. IEEE, 2012.

[12] J. Gao, G. Zhu, E. Strangas, and F. Sun. Equivalent fuel consumption optimal control of a series hybrid electric vehicle. *Proceedings of the Institution of Mechanical Engineers, Part D: Journal of Automobile Engineering*, 223(8):1003–1018, 2009.